Liu *et al. Horticulture Advances* (2026) 4:16
https://doi.org/10.1007/s44281-026-00105-x

Horticulture Advances

RESEARCH ARTICLE Open Access

Ca^{2+} deficiency disrupts ROS homeostasis and induces tip burn in Chinese cabbage

Hong Liu[1], Guoqing Du[1], Haowen Cai[1], Shigeng Ma[1], Mengting Mao[1], Xijiao Kang[1] and Shanshan Nie[1*]

Abstract

Ca^{2+} deficiency causes irreversible physiological disorders that markedly reduce the yield and quality of many horticultural crops, leading to substantial economic losses. Tip burn in Chinese cabbage (*Brassica rapa* ssp. *pekinensis*) is associated with Ca^{2+} deficiency; however, the underlying molecular mechanisms remain poorly understood. In this study, Ca^{2+} deficiency suppressed growth and impaired photosynthetic performance in Chinese cabbage seedlings. Under Ca^{2+} deficiency, cytosolic Ca^{2+} levels decreased, accompanied by excessive reactive oxygen species (ROS) accumulation in the leaves. Foliar application of dimethylthiourea (DMTU), an ROS scavenger, alleviated Ca^{2+} deficiency-induced tip burn by reducing ROS accumulation. RNA-seq analysis further revealed significant enrichment of the mitogen-activated protein kinase signaling and plant hormone signal transduction pathways during tip-burn development. Several differentially expressed genes associated with these pathways were identified as responsive to Ca^{2+} deficiency. Compared with normal Ca^{2+} and DMTU-rescued conditions, the *respiratory burst oxidase homolog D* (*BrRbohD-2*) gene was markedly upregulated under Ca^{2+} deficiency. Overexpression of *BrRbohD-2* increased ROS accumulation and aggravated tip burn in Chinese cabbage seedlings, whereas its suppression reduced ROS levels and alleviated tip burn. These findings provide important insights into the role of *BrRbohD-2* and the regulatory mechanisms underlying Ca^{2+} deficiency-related disorders in *Brassicaceae* crops.

Keywords Chinese cabbage, Ca^{2+} deficiency stress, Tip burn, *BrRbohD-2* gene, RNA-seq

Introduction

Calcium (Ca^{2+}) is an essential macronutrient for plants and plays critical roles in various aspects of plant growth, development, and responses to abiotic stresses (White and Broadley 2003; McAinsh and Pittman 2009; Swarbreck et al. 2013). Ca^{2+} deficiency induces irreversible physiological disorders that significantly reduce yield and quality, leading to substantial economic losses in many horticultural crops (White and Broadley 2003; McAinsh and Pittman 2009). Common manifestations include bitter pit in apples (Torres et al. 2024), blossom-end rot in tomatoes (Ho and White 2005), black heart in celery (Aloni and Pressman 1987), and tip burn in leafy vegetables (Kuronuma and Watanabe 2021). Ca^{2+} deficiency is associated with complex interactions among mineral elements and environmental factors, which disrupt Ca^{2+} uptake and transport, create unfavorable growth conditions, and result in uncoordinated plant development (White and Broadley 2003; Kuronuma et al. 2020). These deficiency-related disorders are often linked to a decrease in cytosolic Ca^{2+} levels below a critical threshold, especially in rapidly growing tissues (Kuronuma and Watanabe 2021; Torres et al. 2024).

Leafy vegetables are particularly susceptible to Ca^{2+} deficiency stress and frequently exhibit tip-burn symptoms, including small black spots on petioles, necrosis at leaf margins, lesion formation, new curling, shrinking, and wilting of young leaves (Li et al. 2022, 2023; Cui et al. 2023). Studies on Chinese cabbage (*Brassica rapa* ssp. *pekinensis*) have shown that localized Ca^{2+} deficiency

*Correspondence:
Shanshan Nie
niess@nwafu.edu.cn
[1] College of Horticulture, Northwest A&F University, Yangling 712100, People's Republic of China

© The Author(s) 2026. **Open Access** This article is licensed under a Creative Commons Attribution 4.0 International License, which permits use, sharing, adaptation, distribution and reproduction in any medium or format, as long as you give appropriate credit to the original author(s) and the source, provide a link to the Creative Commons licence, and indicate if changes were made. The images or other third party material in this article are included in the article's Creative Commons licence, unless indicated otherwise in a credit line to the material. If material is not included in the article's Creative Commons licence and your intended use is not permitted by statutory regulation or exceeds the permitted use, you will need to obtain permission directly from the copyright holder. To view a copy of this licence, visit http://creativecommons.org/licenses/by/4.0/.

Springer

in the developing leaf apex, leading to insufficient Ca^{2+} supply, is a major cause of tip burn (Su et al. 2019). At the cellular level, Ca^{2+} is primarily stored in various organelles, with the vacuole and endoplasmic reticulum (ER) serving as major reservoirs (Stael et al. 2012; Costa et al. 2018). The dynamic regulation of intracellular Ca^{2+} levels is essential for rapid responses to environmental stimuli and for determining stress resistance (Wang and Luan 2024). These fluctuations are controlled by Ca^{2+} transport and storage systems involving diverse Ca^{2+} transporters, channels, signaling components, and Ca^{2+}-binding proteins (Berridge et al. 2003; Kudla et al. 2010; He et al. 2021). Among these, well-characterized Ca^{2+} transporters include plasma membrane-localized autoinhibited Ca^{2+}-ATPase (ACAs), vacuolar calcium-proton exchangers (CAXs), and ER calcium ATPase (ECA), which collectively regulate Ca^{2+} efflux to maintain cytosolic Ca^{2+} homeostasis (Robertson 2013; Ma and Berkowitz 2017). In contrast, cyclic nucleotide-gated ion channels (CNGCs) facilitate Ca^{2+} influx and are recognized as key components in early signaling events (Yang et al. 2024). The coordinated activity of these channels and transporters underpins Ca^{2+} signaling and is critical for maintaining cytosolic Ca^{2+} homeostasis (Bose et al. 2014; Wang and Luan 2024).

Different environmental stimuli can induce changes in the cytosolic Ca^{2+} concentration and also alter reactive oxygen species (ROS) homeostasis (Kadota et al. 2015; Nadarajah 2020). ROS are key signaling molecules that function in a variety of plant processes, including the induction of Ca^{2+} cascades, stress perception, and signal transduction (Ali et al. 2023; Ravi et al. 2023). Most ROS are generated by plant NADPH oxidases, also known as respiratory burst oxidase homolog (RBOH) proteins. However, excessive accumulation of excess ROS leads to oxidative stress and damages essential biomolecules (Chapman et al. 2019; Li et al. 2019). Therefore, maintaining ROS homeostasis is critical for preventing oxidative damage and enabling adaptive responses to environmental stresses (Chapman et al. 2019; Ali et al. 2023). The interplay between ROS and Ca^{2+} signaling primarily involves Ca^{2+} channels, Ca^{2+} sensors, and RBOHs, including the highly expressed RBOHD, which is regulated by Ca^{2+} through direct binding to EF-hand motifs (Kadota et al. 2015; Ali et al. 2023; Ravi et al. 2023). The model plant *Arabidopsis thaliana* contains 10 RBOH family members, and studies have shown that different RBOHs play distinct roles in regulating various biological processes (Kadota et al. 2015; Chapman et al. 2019). For instance, RBOHD and RBOHF are major contributors to ROS production in response to multiple abiotic stresses (Zhai et al. 2018), while a specific role for RBOHD has been reported under iron deficiency (Miller et al. 2009). Additionally, ROS participate in the activation of the mitogen-activated protein kinase (MAPK) cascade, a central signaling pathway that transduces extracellular stimuli into intracellular responses during environmental stress (Jalmi and Sinha 2015; Niekerk et al. 2024). However, the specific molecular mechanisms underlying Ca^{2+} deficiency-induced ROS signaling that initiate and regulate tip burn in Chinese cabbage remain largely unexplored.

Therefore, the objectives of this study were to evaluate the physiological effects of Ca^{2+} deficiency-induced tip burn and to investigate the role of ROS accumulation under Ca^{2+} deficiency in Chinese cabbage. A systematic analysis was conducted to assess disease progression, cytosolic Ca^{2+} levels, ROS accumulation, and the expression of the ROS-producing gene *BrRbohD-2* in leaves exhibiting tip-burn symptoms. Furthermore, the pivotal role of *BrRbohD-2*-dependent ROS production in mediating tip burn under Ca^{2+} deficiency was validated through overexpression and gene-silencing experiments. This study provides novel molecular insights into the mechanisms underlying Ca^{2+} deficiency-induced disorders in Chinese cabbage and other crops.

Materials and methods

Plant materials and treatments

Two high-generation inbred lines of Chinese cabbage, the tip-burn-susceptible line '10S42' and the resistant line '10S27' (Cui et al. 2023), were used for Ca^{2+} deficiency treatment and tip-burn phenotype analysis. Germinated seeds were grown in 1/4-strength Hoagland nutrient solution under standard growth conditions for 7 d. The seedlings were then transferred to full-strength Hoagland nutrient solution until the second true leaf was fully expanded. The seedlings were cultivated in a controlled growth chamber under a 16 h light (24 °C, 216 $\mu mol \cdot m^{-2} \cdot s^{-1}$)/8 h dark (16 °C) photoperiod with 55% relative humidity (Huo et al. 2024). For Ca^{2+}-deficiency treatments, seedlings were exposed to Hoagland solutions containing 0.75, 0.5, and 0.25 mM Ca^{2+}. These concentrations were selected based on preliminary experiments and a previous report (Cui et al. 2023). A normal Hoagland solution containing 4 mM Ca^{2+} was used as the control. The disease index (DI) and severity of tip burn were assessed based on the rating criteria described by Li et al. (2023). Ca^{2+} fertilizer supplementation is a common agricultural practice used to prevent tip burn during the growth of Chinese cabbage. To evaluate mitigation strategies, seedlings subjected to Ca^{2+} deficiency (0.25 mM Ca^{2+}) were sprayed with 25 mM $CaCl_2$ solution as a positive

control to alleviate tip burn, while distilled water was used as a control treatment. In addition, seedlings were sprayed with 1 mM dimethylthiourea (DMTU), a scavenger of H_2O_2 and $O_2^{\bullet-}$, to assess its effect on tip burn. Each seedling was sprayed with 1 mL of solution once every 2 d.

Determination of physiological parameters

The maximum leaf area of seedlings was measured using a portable laser leaf area meter (Win FOLIA, REGENT Instruments Inc., Quebec City, Canada). Root activity was determined following the method of Onanuga and Adl (2012). Chlorophyll and carotenoid contents were measured using a spectrophotometer (Infinite M200 PRO, Tecan Group Ltd., Männedorf, Switzerland), at 470, 649, and 665 nm, as previously described (Huo et al. 2024). The net photosynthetic rate (Pn), stomatal conductance (Gsw), transpiration rate (E), and intercellular CO_2 concentration (Ci) were measured using an LI-6800 portable photosynthesis system (LI-COR Biosciences, Lincoln, Nebraska, USA). Chlorophyll fluorescence parameters, including the maximum quantum yield of PSII (Fv/Fm), effective photochemical efficiency [Y(Ⅱ)], photochemical quenching coefficient (qP), and non-photochemical quenching (NPQ), were determined using a Dual-PAM-100 chlorophyll fluorometer (Heinz Walz GmbH, Effeltrich, Germany). Histochemical staining was performed to detect H_2O_2 and $O_2^{\bullet-}$ accumulation using 3,3′-diaminobenzidine (DAB) and nitroblue tetrazolium (NBT), respectively. Malondialdehyde (MDA) content and H_2O_2 levels were quantified using commercial assay kits (Suzhou Comin Biotechnology Co., Ltd., Suzhou, China) according to the manufacturer's instructions, with measurements taken on a microplate reader (Multiskan Spectrum, Thermo Scientific, Waltham, MA, USA).

Measurement of total Ca^{2+} and Mn^{2+} contents and cytosolic Ca^{2+} levels

Heart leaf samples from Ca^{2+}-deficient plants were prepared according to the method described by Cui et al. (2023) and used to determine total Ca^{2+} and Mn^{2+} contents following the procedure of Bai et al. (2023). To assess cytosolic Ca^{2+} levels, samples were washed three times with phosphate-buffered saline (PBS) solution and then incubated in 15 μM Fluo-4 acetoxymethyl ester (AM) solution for 2 h in the dark. The green fluorescence signal was observed using a confocal laser scanning microscope (Leica TCS SP8, Leica Microsystems, Wetzlar, Germany) with excitation and emission wavelengths of 488 and 530 nm, respectively. ImageJ software was used to quantify the gray values of the green fluorescence.

RNA-seq analysis

After 20 d of Ca^{2+} deficiency treatment, heart leaf apex samples from '10S42' were collected and sent to Genedenovo Biotechnology Co., Ltd. (Guangzhou, China) for RNA-seq analysis. cDNA libraries corresponding to the NC (normal, 4 mM Ca^{2+}), DC (0.25 mM Ca^{2+} deficiency), and DCDM (0.25 mM Ca^{2+} deficiency with DMTU treatment) groups were constructed. Three biological replicates were included for each treatment. Clean reads were mapped to the Chinese cabbage reference genome (V3.1; https://brassicadb.cn). Gene expression levels were quantified as transcripts per million (TPM). Differentially expressed genes (DEGs) were defined based on the criteria $|\log_2\text{fold change}| \geq 1$ and FDR < 0.05. Functional annotation and enrichment analyses were performed using the Gene Ontology (GO) and Kyoto Encyclopedia for Genes and Genomes (KEGG) databases with a significance threshold of P values ≤ 0.05. Bioinformatics analyses were performed using Omicsmart (https://www.omicsmart.com), an online platform for interactive data analysis.

Transient overexpression of *BrRbohD-2* in Chinese cabbage leaves

The *BrRbohD-2* coding sequence was cloned into the pCAMBIA-2300 vector fused with the green fluorescent protein (GFP) reporter and introduced into *Agrobacterium tumefaciens* strain GV3101. For transient expression analysis, *Agrobacterium* GV3101 cells harboring the CaMV35Spro::*BrRbohD-2*-GFP construct (or CaMV35Spro::GFP as a control) were cultured overnight and resuspended in induction medium (10 mM MES, 10 mM $MgCl_2$, and 200 μM acetosyringone; pH 5.6) to an OD_{600} of 1.0. Approximately 1 mL of the suspension was infiltrated into the leaves of Chinese cabbage at the two-leaf stage using a syringe. After 24 h, the seedlings were treated with Ca^{2+}-deficient Hoagland solution (0.1 mM Ca^{2+}) and incubated in the dark for 2 d. Leaves infiltrated with the empty vector strain or ddH_2O were used as controls. GFP fluorescence was observed using a confocal laser scanning microscope (Leica TCS SP8) to confirm successful infiltration. The infiltrated leaves were subsequently collected for further analysis.

Virus-induced gene silencing (VIGS) of *BrRbohD-2* in Chinese cabbage

In accordance with the method described by Xiao et al. (2020), a VIGS system based on cabbage leaf crumple virus (CaLCuV) was employed. A 500 bp fragment from each of *BrRbohD-2* and phytoene desaturase (*BrPDS*; BraA04g007910.3C) was cloned into the PCVA vector. Subsequently, *Agrobacterium* suspensions containing PCVB were mixed with those harboring PCVA,

PCVA-*BrRbohD-2*, or PCVA-*BrPDS*, resulting in three infiltration treatments: PCVA/PCVB (control), PCVA-*BrRbohD-2*/PCVB, and PCVA-*BrPDS*/PCVB (positive control, which produces a photobleaching phenotype following gene silencing). Germinated seeds with approximately 1 cm radicles were immersed in the infection mixture and subjected to vacuum infiltration at −0.08 MPa for 20 min. The seeds were then planted in soil and grown under normal conditions. PCVA-*BrRbohD-2*/PCVB seedlings at the two-leaf stage were selected based on the photobleaching phenotype observed in the PCVA-*BrPDS*/PCVB plants and used for subsequent Ca^{2+} deficiency treatment (0.1 mM Ca^{2+}).

Quantitative real-time PCR (RT-qPCR)

Total RNA extraction, cDNA synthesis, and RT-qPCR analysis were performed as described by Nie et al. (2019). RT-qPCR was conducted using an IQ5 Real-Time PCR Detection System (Bio-Rad Laboratories, Hercules, CA, USA). Specific primers were designed using Primer Premier 5 software (Table S1). Relative gene expression levels were calculated using the $2^{-\Delta\Delta CT}$ method. Each sample was analyzed with three biological replicates, and each biological replicate included three technical replicates.

Statistical analysis

Statistical analyses were performed using one-way analysis of variance (ANOVA) followed by Duncan's multiple range test in SPSS 26.0 software. Data are presented as means ± SEMs ($P < 0.05$). Correlations between tip-burn severity and 23 physiological indices were evaluated using Pearson's correlation analysis. A radar chart was used for comprehensive analysis of multiple indices.

Results

Effects of Ca^{2+} deficiency stress on tip-burn occurrence and growth in Chinese cabbage

To investigate the effects of Ca^{2+} deficiency on tip-burn occurrence in Chinese cabbage, seedlings of '10S27' and '10S42' were subjected to different Ca^{2+} concentrations. As the Ca^{2+} concentration decreased, tip-burn severity and DI increased in both lines (Fig. 1a, b), whereas shoot and root fresh weights decreased progressively (Fig. 1c, d). Root length, root activity, and maximum leaf area also showed a gradual decline (Fig. S1). These results indicate that Ca^{2+} deficiency significantly induces tip burn and inhibits growth in Chinese cabbage seedlings. After 20 d of treatment under 0.25 mM Ca^{2+}, the DI was significantly greater in '10S42' than in '10S27' (Fig. 1e),

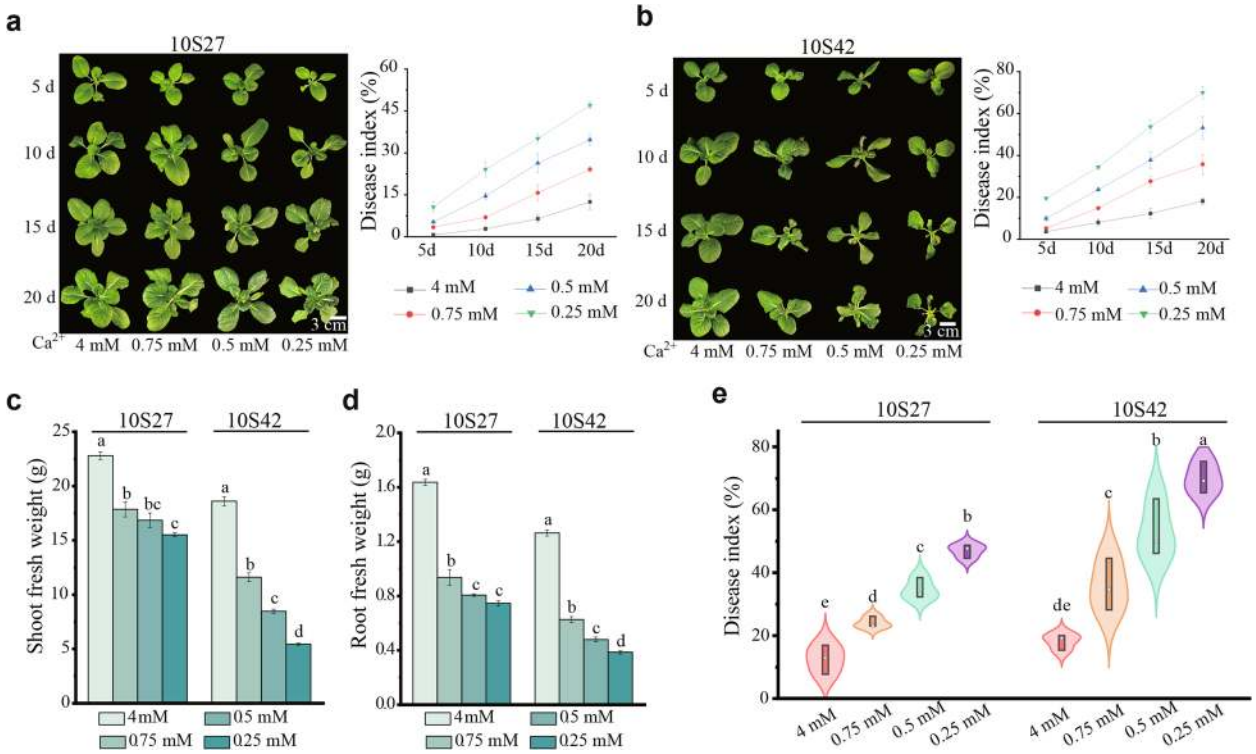


Fig. 1 Observation of tip burn in Chinese cabbage lines '10S27' and '10S42' under Ca^{2+} deficiency. **a** Phenotype and disease index (DI) of tip burn in '10S27' seedlings. **b** Phenotype and DI of tip burn in '10S42' seedlings. **c** Shoot fresh weight. **d** Root fresh weight. **e** DI at 20 d under 0.25 mM Ca^{2+} deficiency conditions. Scale bar = 3 cm (**a**, **b**). Different letters indicate significant differences at $P < 0.05$. Data are presented as the mean ± SEM of three independent replicates

indicating that '10S42' is sensitive, whereas '10S27' is tolerant to Ca^{2+} deficiency-induced tip burn.

Phenotypic analysis of heart leaves revealed that tip-burn symptoms, including withered leaf margins, leaf curling, and leaf shrinkage and wilting, were observed in both '10S27' and '10S42' under Ca^{2+} deficiency stress, with symptoms being most severe at 0.25 mM Ca^{2+} (Fig. 2a). Moreover, as the Ca^{2+} concentration decreased, total chlorophyll and carotenoid contents declined in a concentration-dependent manner in both lines (Fig. 2b). Measurements of photosynthetic parameters showed that Pn, E, and Gsw decreased progressively, whereas Ci increased (Fig. 2c). Under Ca^{2+}-deficient conditions, Fv/Fm, Y(II), and qP also decreased, whereas NPQ increased in both lines (Fig. 2d). These results indicate that Ca^{2+} deficiency-induced tip burn severity is closely associated with reduced photosynthetic performance in Chinese cabbage.

Ca^{2+} deficiency affects Ca^{2+} and Mn^{2+} contents and reduces cytosolic Ca^{2+} levels in leaves

In this study, the concentrations of major macronutrient cations (Ca^{2+} and Mn^{2+}) in the roots, outer leaf apex, and heart leaf apex were measured under Ca^{2+}-deficient conditions. The contents of both Ca^{2+} and Mn^{2+} decreased in different tissues of '10S27' and '10S42' seedlings with different Ca^{2+} concentrations (Table 1). Under 0.25 mM Ca^{2+} treatment, the total contents of Ca^{2+} and Mn^{2+} were the highest in the roots, followed by the outer leaf apex, and the lowest in the heart leaf apex in both lines (Fig. 3a, b). Moreover, the total Ca^{2+} content in the heart leaf apex of '10S27' was significantly higher than that in '10S42' under 0.25 mM Ca^{2+} treatment (Fig. 3a), whereas the total Mn^{2+} content did not differ significantly between the two lines (Fig. 3b).

Furthermore, cytosolic Ca^{2+} levels in heart leaves exhibiting tip-burn symptoms were assessed. Cytosolic

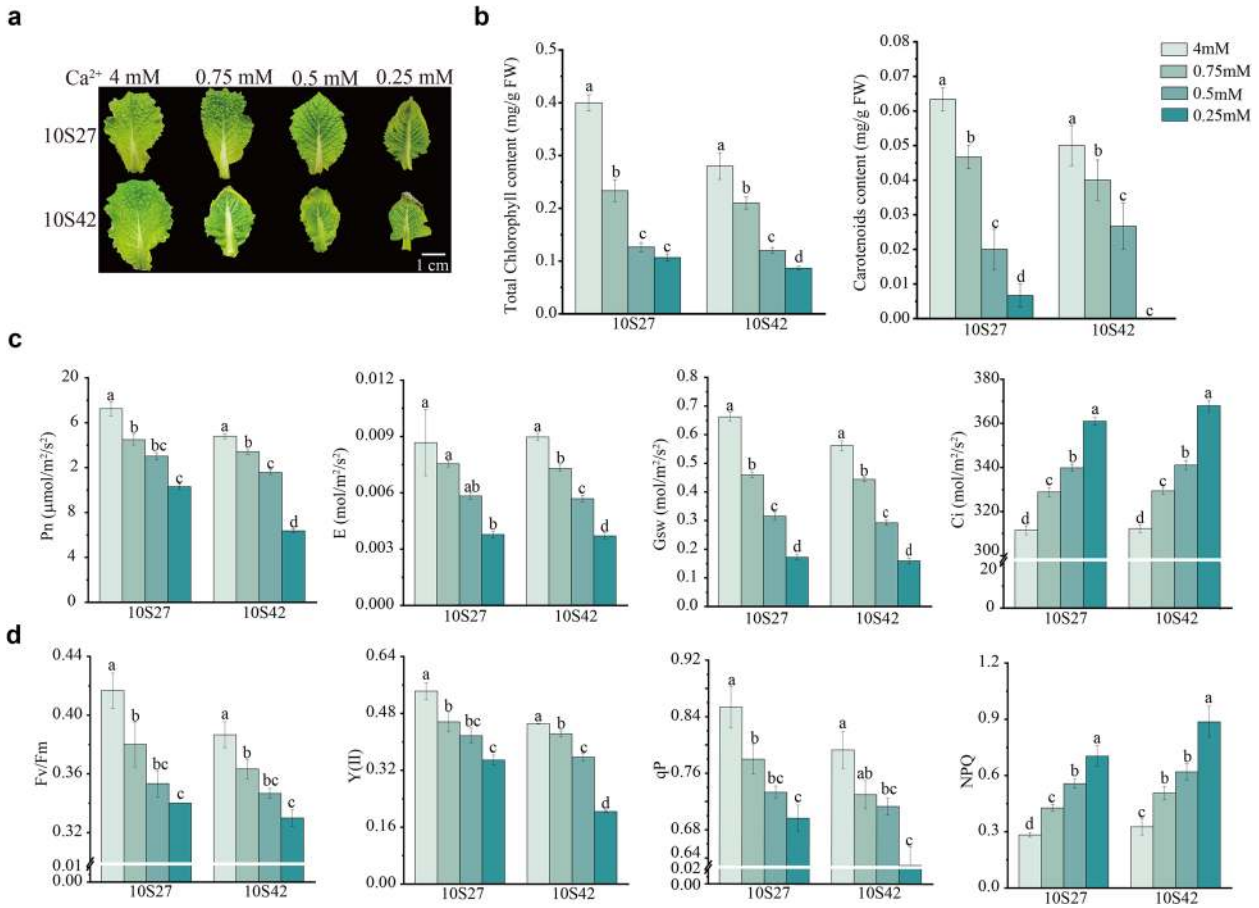


Fig. 2 Effects of Ca^{2+} deficiency stress on the photosynthetic performance of Chinese cabbage leaves. **a** Tip-burn phenotype of heart leaves. **b** Chlorophyll and carotenoid contents. FW, fresh weight. Scale bar = 1 cm. **c** Net photosynthetic rate (Pn), transpiration rate (E), stomatal conductance (Gsw), and intercellular CO_2 concentration (Ci) values. **d** Maximum quantum efficiency of PSII (Fv/Fm), effective quantum yield of PSII [Y(II)], photochemical quenching (qP), and non-photochemical quenching (NPQ) values. Different letters indicate significant differences at $P < 0.05$. Data are presented as the mean ± SEM of three independent replicates

Table 1 Total Ca^{2+} and Mn^{2+} contents in different tissues of Chinese cabbage under Ca^{2+} deficiency conditions

Tissue	Ca^{2+} deficiency condition	10S27		10S42	
		Ca^{2+}/mg·g^{-1} DW	Mn^{2+}/μg·g^{-1} DW	Ca^{2+}/mg·g^{-1} DW	Mn^{2+}/μg·g^{-1} DW
Root	4 mM	5.145 ± 0.264a	0.278 ± 0.012a	4.336 ± 0.020a	0.260 ± 0.002a
	0.75 mM	2.713 ± 0.115b	0.243 ± 0.004b	2.035 ± 0.005b	0.225 ± 0.010b
	0.5 mM	1.711 ± 0.078c	0.213 ± 0.003c	1.571 ± 0.015c	0.179 ± 0.004c
	0.25 mM	1.567 ± 0.073c	0.160 ± 0.006d	1.317 ± 0.092d	0.144 ± 0.006d
Outer leaf apex	4 mM	16.060 ± 0.522a	0.348 ± 0.002a	13.383 ± 0.038a	0.296 ± 0.001a
	0.75 mM	6.285 ± 0.268b	0.282 ± 0.003b	4.224 ± 0.043b	0.211 ± 0.002b
	0.5 mM	2.879 ± 0.090c	0.203 ± 0.004c	2.082 ± 0.075c	0.159 ± 0.006c
	0.25 mM	1.466 ± 0.416d	0.130 ± 0.007d	1.130 ± 0.092d	0.123 ± 0.003d
Heart leaf apex	4 mM	5.077 ± 0.037a	0.260 ± 0.004a	5.077 ± 0.037a	0.164 ± 0.001a
	0.75 mM	3.143 ± 0.146b	0.153 ± 0.004b	2.156 ± 0.005b	0.130 ± 0.001b
	0.5 mM	1.677 ± 0.089c	0.131 ± 0.001c	1.370 ± 0.006c	0.115 ± 0.002c
	0.25 mM	1.506 ± 0.035c	0.086 ± 0.001d	0.972 ± 0.010d	0.081 ± 0.002d

'10S42' (tip-burn-susceptible) and '10S27' (resistant), high-generation inbred lines of Chinese cabbage; DW, dry weight

Ca^{2+} levels decreased in both lines under Ca^{2+} deficiency (Fig. 3c, d). Under 0.25 mM Ca^{2+} treatment, the heart leaf apex of '10S42' exhibited significantly weaker Ca^{2+} fluorescence signals than that of '10S27' (Fig. 3c, d). In contrast, as the Ca^{2+} concentration decreased, cytosolic Ca^{2+} levels in the root tips increased significantly (Fig. 3e, f), which may be associated with reduced root activity under Ca^{2+} deficiency. The differential changes in cytosolic Ca^{2+} levels between roots and leaves may lead to increased accumulation of cytosolic Ca^{2+} in roots, but insufficient Ca^{2+} supply to the upper leaves, especially the heart leaves, resulting in more pronounced tip-burn symptoms.

Ca^{2+} deficiency-induced tip burn is closely correlated with excessive ROS accumulation in leaves

Under Ca^{2+} deficiency stress, MDA and H_2O_2 contents increased progressively in the heart leaf apex of both lines, which was consistent with the increase in tip-burn DI (Fig. 4a, b). Histochemical staining further revealed more intense NBT and DAB staining in heart leaves under Ca^{2+}-deficient conditions, indicating increased accumulation of $O_2^{\bullet-}$ and H_2O_2, respectively (Fig. 4c). Moreover, staining intensity was the highest under 0.25 mM Ca^{2+} treatment and was significantly greater in '10S42' than in '10S27' (Fig. 4c).

Comprehensive analysis of the 24 indices in response to Ca^{2+} deficiency in both lines was performed using radar charts. Higher values of DI, H_2O_2, MDA, Ci, and NPQ were exhibited in '10S42' across all treatments, whereas lower values of Pn, Fv/Fm, qP, and related parameters were detected in '10S42.' These analyses clearly revealed differences in susceptibility between '10S27' and '10S42' (Fig. 4d). Pearson correlation analysis showed that tip-burn DI was most strongly correlated with H_2O_2 (r = 0.9384) and MDA (r = 0.9361), followed by root activity (r = –0.9312), Fv/Fm (r = –0.9288), NPQ (r = 0.9144), and Pn (r = –0.9141) (Fig. 4e). These results indicate that Ca^{2+} deficiency-induced tip-burn severity is closely associated with excessive ROS accumulation in leaves.

Exogenous application of DMTU alleviates Ca^{2+} deficiency-induced tip burn

To further examine whether ROS accumulation is directly associated with Ca^{2+} deficiency-induced tip burn in Chinese cabbage, foliar application of $CaCl_2$ and DMTU (an H_2O_2 and $O_2^{\bullet-}$ scavenger) was performed in '10S42' under 0.25 mM Ca^{2+} deficiency stress. Following $CaCl_2$ and DMTU treatments, tip-burn symptoms were almost completely absent, and the DI was significantly reduced (Fig. 5a, b). Compared with the Ca^{2+}-deficient group, shoot fresh weight, Pn, and Fv/Fm increased in the DMTU-treated group, whereas NPQ decreased significantly (Fig. 5c, d). $CaCl_2$ treatment resulted in the highest values of shoot fresh weight, Pn, and Fv/Fm and the lowest NPQ (Fig. 5c, d). Furthermore, both $CaCl_2$ and DMTU treatments significantly increased cytosolic Ca^{2+} levels in heart leaves (Fig. 5e). Consistently, $CaCl_2$- and DMTU-treated seedlings showed the least intense NBT and DAB staining in heart leaves, indicating reduced accumulation of H_2O_2 and $O_2^{\bullet-}$ (Fig. 5f, g). Similar trends were observed in '10S27' (Fig. S2). These findings indicate that DMTU application reduces excess ROS and alleviates Ca^{2+} deficiency-induced tip burn in Chinese cabbage seedlings.

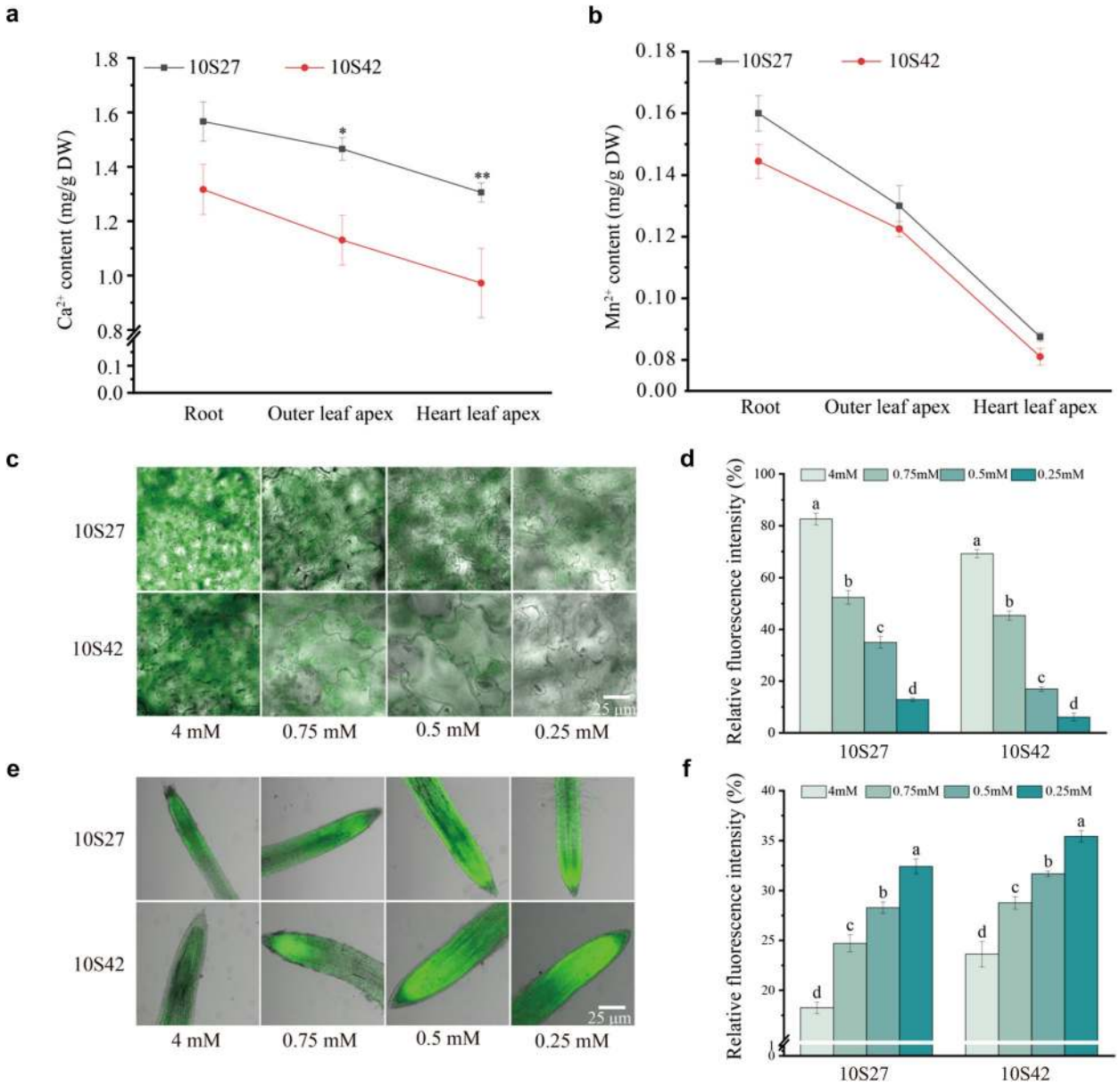


Fig. 3 Total Ca^{2+} and Mn^{2+} contents and cytosolic Ca^{2+} levels in Chinese cabbage seedlings under Ca^{2+} deficiency. **a, b** Total Ca^{2+} contents (**a**) and total Mn^{2+} contents (**b**) in the root, outer leaf apex, and heart leaf apex at 20 d after 0.25 mM Ca^{2+} deficiency treatment. DW, dry weight. * $P < 0.05$, ** $P < 0.01$. **c, d** Cytosolic Ca^{2+} levels in the heart leaf apex. Green fluorescence signal (**c**) and relative fluorescence intensity (**d**). **e, f** Cytosolic Ca^{2+} levels in roots. Green fluorescence signal (**e**) and relative fluorescence intensity (**f**). Scale bar = 25 μm (**c**, **e**). Different letters indicate significant differences at $P < 0.05$. Data are presented as the mean ± SEM of three independent replicates

RNA-seq analysis of DMTU-mediated alleviation of Ca^{2+} deficiency-induced tip burn in Chinese cabbage

To investigate the molecular mechanism by which DMTU alleviates Ca^{2+} deficiency-induced tip burn, nine cDNA libraries were constructed from the heart leaf apex of '10S42' under normal conditions (NC), Ca^{2+} deficiency conditions (DC), and Ca^{2+} deficiency with DMTU treatment (DCDM), with three biological replicates (Fig. 6a). The number of clean reads ranged from 35.01 to 40.10 million across the libraries, with GC contents of 46.99–47.76% and Q30 values of 91.40–93.73% (Table S2). The reads were mapped to the Chinese cabbage reference genome with an average mapping efficiency ranging from 86.88% to 89.22% (Table S2). Differential expression analysis identified 3540 DEGs in the NC *vs* DC comparison (3013 upregulated and 527 downregulated), 2594 DEGs in the DC *vs* DCDM comparison (302 upregulated and 2292

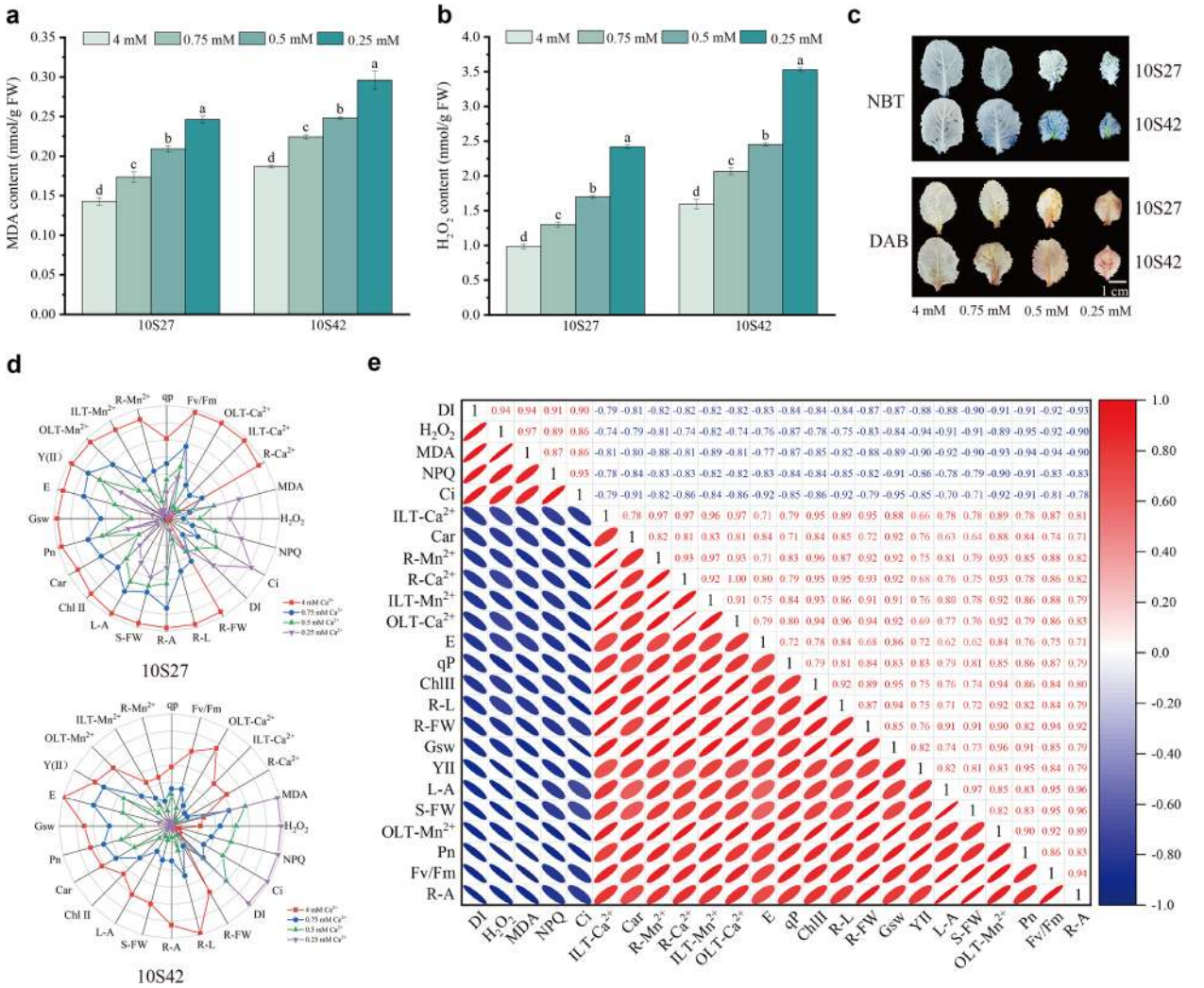


Fig. 4 Effects of Ca^{2+} deficiency on reactive oxygen species (ROS) accumulation in Chinese cabbage leaves. **a** Malondialdehyde (MDA) content. FW, fresh weight. **b** Hydrogen peroxide content (H_2O_2) content. **c** Histochemical staining with nitroblue tetrazolium (NBT) and 3,3′-diaminobenzidine (DAB). Scale bar = 1 cm. **d** Radar chart of 24 tip-burn-related indices in '10S27' and '10S42'. DI, disease index; NPQ, non-photochemical quenching; Ci, intercellular CO_2 concentration; ILT-Ca^{2+}, inner leaf tip Ca^{2+}; Car, carotenoid; R-Mn^{2+}, root Mn^{2+}; R-Ca^{2+}, root Ca^{2+}; ILT-Mn^{2+}, inner leaf tip Mn^{2+}; QLT-Ca^{2+}, outer leaf tip Ca^{2+}; E, transpiration rate; qP, coefficient photochemical quenching; ChlII, Chlorophyll; R-L, root length; R-FW, root fresh weight; Gsw, stomatal conductance; YⅡ, effective quantum yield of PSII; L-A, leaf angle; S-FW, shoot fresh weight; QLT-Mn^{2+}, outer leaf tip Mn^{2+}; Pn, net photosynthetic rate; Fv/Fm, maximum quantum efficiency of PSII; R-A, root activity. **e** Pearson correlation analysis of the 24 indices. Different letters indicate significant differences at $P < 0.05$. Data are presented as the mean ± SEM of three independent replicates

downregulated), and 42 DEGs in the NC *vs* DCDM comparison (23 upregulated and 19 downregulated) (Fig. 6b). Additionally, 12 DEGs were common to all three comparisons. Pairwise overlaps included 2237 common DEGs between NC *vs* DC and DC *vs* DCDM, 15 between DC *vs* DCDM and NC *vs* DCDM, and 28 between NC *vs* DC and NC *vs* DCDM (Fig. 6c).

Functional annotation and enrichment analysis categorized these DEGs into 45, 44, and 26 GO subcategories in the NC *vs* DC, DC *vs* DCDM, and NC *vs* DCDM comparisons, respectively (Fig. S3). Additionally, 3540, 2594, and 42 DEGs were annotated to 128, 116, and 14 KEGG pathways in the comparisons (Fig. S3). The metabolic pathway (ko01100) and biosynthesis of secondary metabolites (ko01110) were significantly enriched across all three comparisons. Furthermore, plant hormone signal transduction (ko04075) and the MAPK signaling pathway (ko04016) were significantly enriched in the NC *vs* DC and DC *vs* DCDM comparisons, but not in the NC *vs* DCDM comparison. These results suggest that DEGs associated with plant hormone and MAPK signaling pathways may play important roles in the regulation of Ca^{2+} deficiency-induced tip burn.

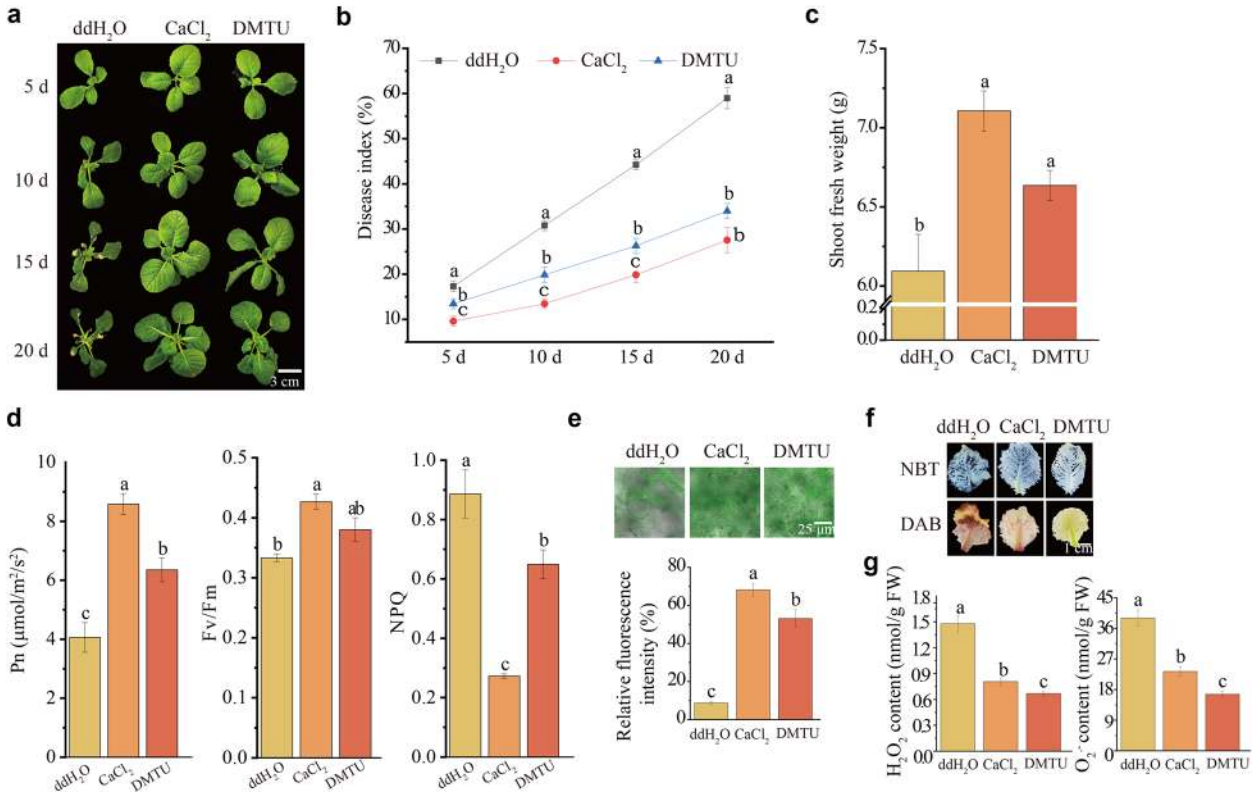


Fig. 5 Effect of dimethylthiourea (DMTU) spraying on Ca^{2+} induced-tip burn in Chinese cabbage. **a** Tip-burn phenotype of seedlings after $CaCl_2$ and DMTU treatment under Ca^{2+} deficiency. **b** Disease index of tip burn. **c** Shoot fresh weight. **d** Net photosynthetic rate (Pn), maximum quantum efficiency of PSII (Fv/Fm), and non-photochemical quenching (NPQ). **e** Cytosolic Ca^{2+} levels in the heart leaf apex. **f** Nitroblue tetrazolium (NBT) and 3,3′-diaminobenzidine (DAB) staining. **g** Hydrogen peroxide (H_2O_2) and superoxide anion ($O_2^{\bullet-}$) contents. FW, fresh weight. Scale bars = 3 cm (**a**), 25 μm (**e**), and 1 cm (**f**). Different letters indicate significant differences at $P < 0.05$. Data are presented as the mean ± SEM of three independent replicates

Analysis of DEGs related to Ca^{2+} signal transduction under Ca^{2+} deficiency stress

Imbalances in Ca^{2+} signal transduction and reductions in cytosolic Ca^{2+} levels may contribute to Ca^{2+} deficiency-induced tip burn (Su et al. 2019; Li et al. 2023). In this study, 32 DEGs encoding Ca^{2+}-binding proteins were upregulated in the NC *vs* DC comparison and downregulated in the DC *vs* DCDM comparison (Fig. 7a; Table S3). Additionally, eight DEGs encoding Ca^{2+} transport-associated proteins were identified, five of which were upregulated in the NC *vs* DC comparison and five were downregulated in the DC *vs* DCDM comparison (Fig. 7b; Table S3). The expression levels of *BrCNGC2*, *BrCNGC4*, and *cation exchanger 1–2* (*BrCAX1-2*) were significantly lower in both the NC *vs* DC and NC *vs* DCDM comparisons (Fig. 7b). To validate the RNA-seq results, eight Ca^{2+}-transport-associated genes were selected for RT-qPCR analysis. The results showed that the expression levels of *BrACA4*, *BrACA11*, *BrCAX1-1*, *BrCAX1-2*, *BrCAX3*, and *BrECA3* was significantly upregulated in DC compared with NC and DCDM, whereas *BrCNGC2* and *BrCNGC4* were significantly downregulated in DC (Fig. 7c). The RT-qPCR results were consistent with the RNA-seq data, except for *BrCAX1-2*, confirming the reliability of the RNA-seq analysis.

Analysis of DEGs related to plant hormone signaling and the MAPK cascade under Ca^{2+} deficiency stress

The enrichment analysis revealed significant enrichment of pathways related to plant hormone signaling and the MAPK cascade in the NC *vs* DC and DC *vs* DCDM comparisons. A total of 17 DEGs involved in the MAPK signaling pathway were upregulated in the NC *vs* DC comparison and downregulated in the DC *vs* DCDM comparison (Fig. 8a; Table S4). Three *BrRBOH* genes—*BrRbohD-1*, *BrRbohD-2*, and *BrRbohF*—were identified as significantly differentially expressed. *BrRbohD-2* (BraA06g037010.3.1C) was also significantly downregulated in the DCDM treatment compared with the NC treatment group, suggesting that it is likely involved in the mechanism by which DMTU alleviates Ca^{2+} deficiency-induced tip burn.

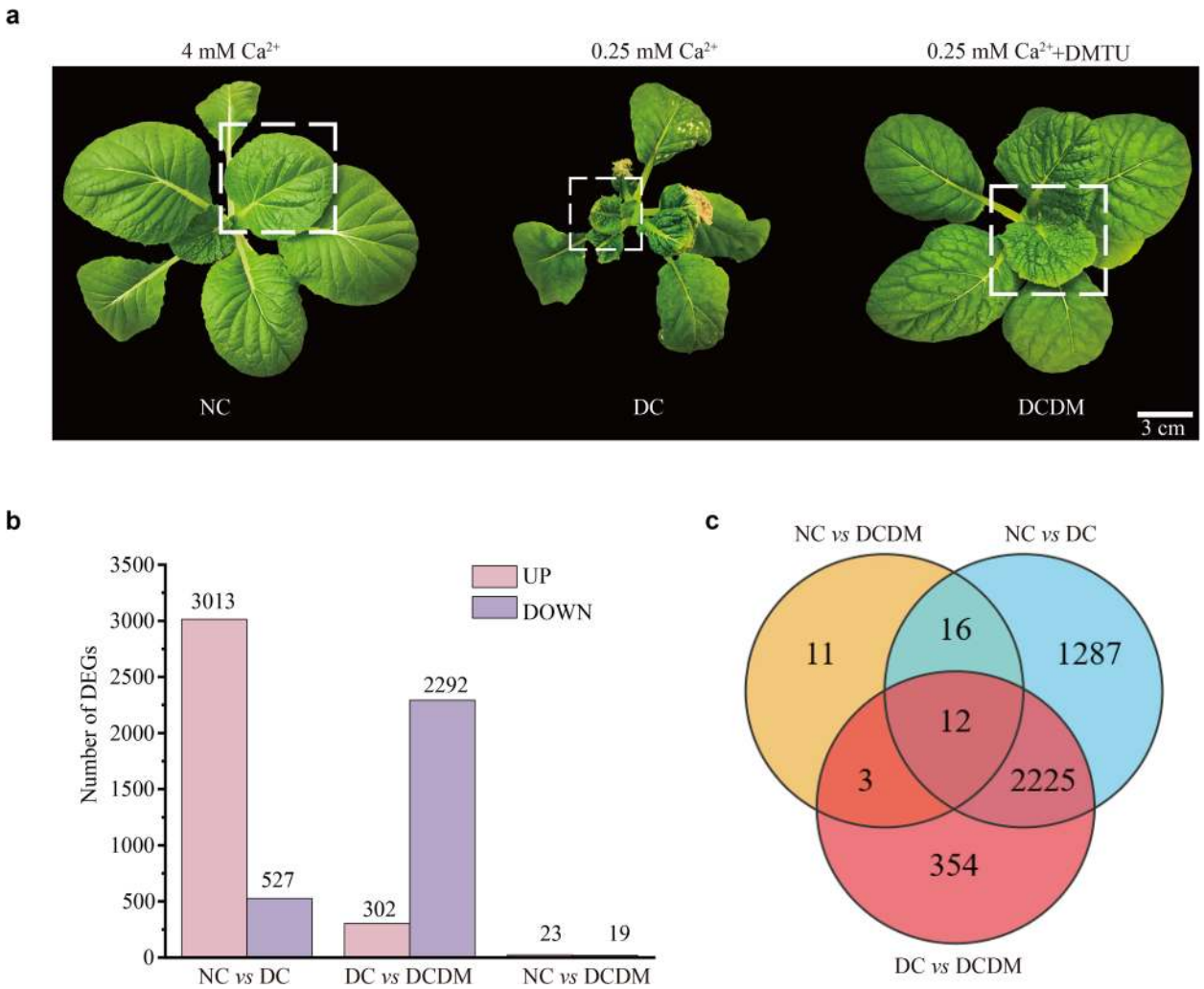


Fig. 6 Identification of differentially expressed genes (DEGs) by RNA-seq analysis in Chinese cabbage. **a** Tip burn phenotype of seedlings under normal conditions (NC), Ca^{2+} deficiency conditions (DC), and Ca^{2+} deficiency with dimethylthiourea (DMTU) treatment (DCDM). Heart leaves (white boxes) were used for cDNA library construction. Scale bar = 3 cm. **b** Numbers of DEGs. **c** Venn diagram showing unique and shared DEGs among different libraries

Additionally, 16 DEGs involved in the plant hormone signal transduction pathway were identified in this study (Fig. 8b; Table S4). The expression of all these DEGs was upregulated in the NC *vs* DC comparison and downregulated in the DC *vs* DCDM comparison. In the NC *vs* DCDM comparison, eight DEGs were upregulated (e.g., pyrabactin resistance 1-like genes *BrPYL6-1* and *BrPYL6-2*), whereas one DEG (*ABA-insensitive 5*, *BrABI5*) was downregulated (Table S4).

Functional analysis of the role of *BrRbohD-2* in regulating Ca^{2+} deficiency-induced tip burn in Chinese cabbage

To further validate the function of *BrRbohD-2* in response to Ca^{2+} deficiency stress, its overexpression (OE-*BrRbohD-2*) and silencing were performed in Chinese cabbage seedlings. The fusion of *BrRbohD-2* with the pCAMBIA2300-GFP vector generated a pCAMBIA2300-*BrRbohD-2* fusion expression construct, which was injected into Chinese cabbage leaves (Fig. 9a). Strong GFP fluorescence and increased *BrRbohD-2* expression were observed in infiltrated leaves (Fig. 9b, c), indicating successful overexpression in OE-*BrRbohD-2* plants. Compared with control plants, OE-*BrRbohD-2* seedlings subjected to Ca^{2+} deficiency (0.1 mM Ca^{2+}) exhibited more severe tip-burn symptoms and higher DI (Fig. 9d, e). Further analysis showed that OE-*BrRbohD-2* leaves exhibited more intense NBT and DAB staining after 8 d of Ca^{2+} deficiency stress (Fig. 9f), indicating increased ROS accumulation. Moreover, cytosolic Ca^{2+} levels (indicated by reduced green fluorescence) were lower in

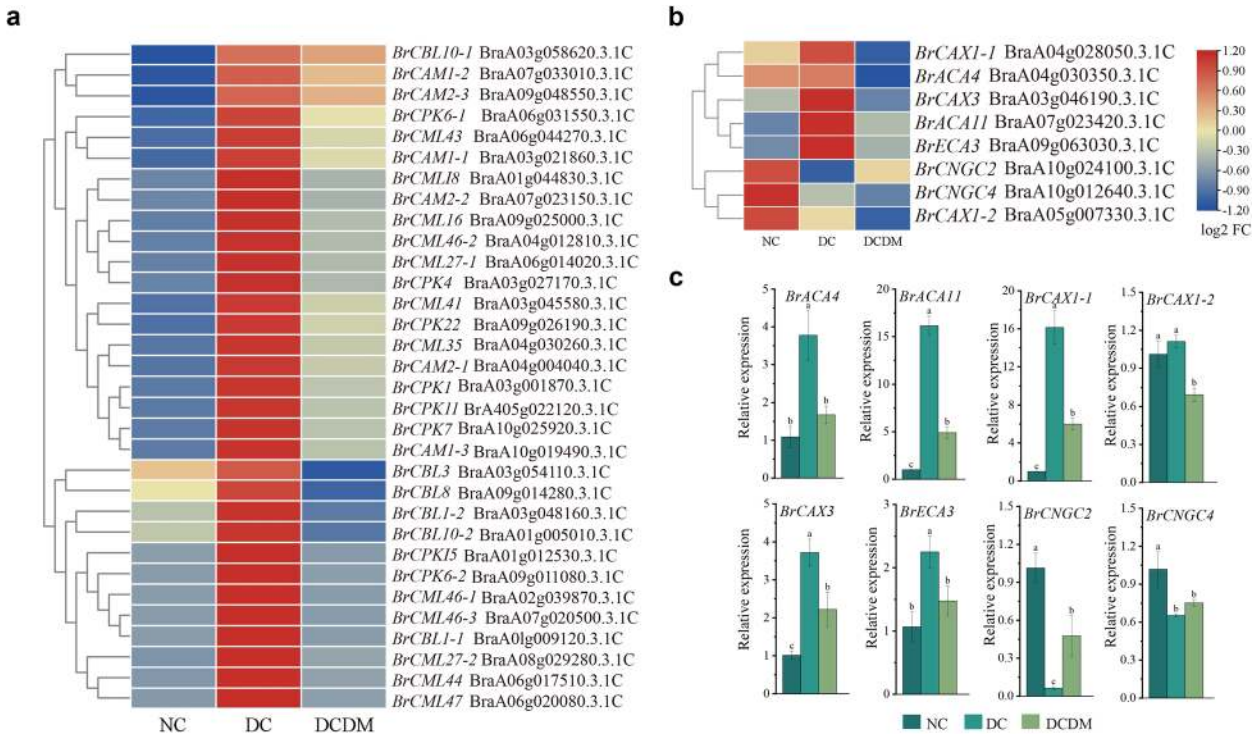


Fig. 7 Heatmap showing expression patterns of differentially expressed genes (DEGs) related to Ca^{2+}-binding proteins (**a**) and Ca^{2+} transport proteins (**b**). Expression values from RNA-seq data are log_2-transformed (log_2fold change, log_2FC) and displayed as color gradients from blue to red. **c** Validation of the expression of eight Ca^{2+} transport-related genes by real time-quantitative PCR (RT-qPCR). Different letters indicate significant differences at $P < 0.05$. *BrCBL*s, *Brassica rapa calcineurin B-like genes*; *BrCAM*s, *calmodulin*; *BrCPK*s, *calcium-dependent protein kinases*; *BrCML*s, *calmodulin-like genes*; *BrCAX*s, *calcium-proton exchangers*; *BrACA*s, *autoinhibited Ca^{2+}-ATPases*; *BrECA, endoplasmic reticulum calcium ATPases*; *BrCNGC*s, *cyclic nucleotide-gated ion channels*

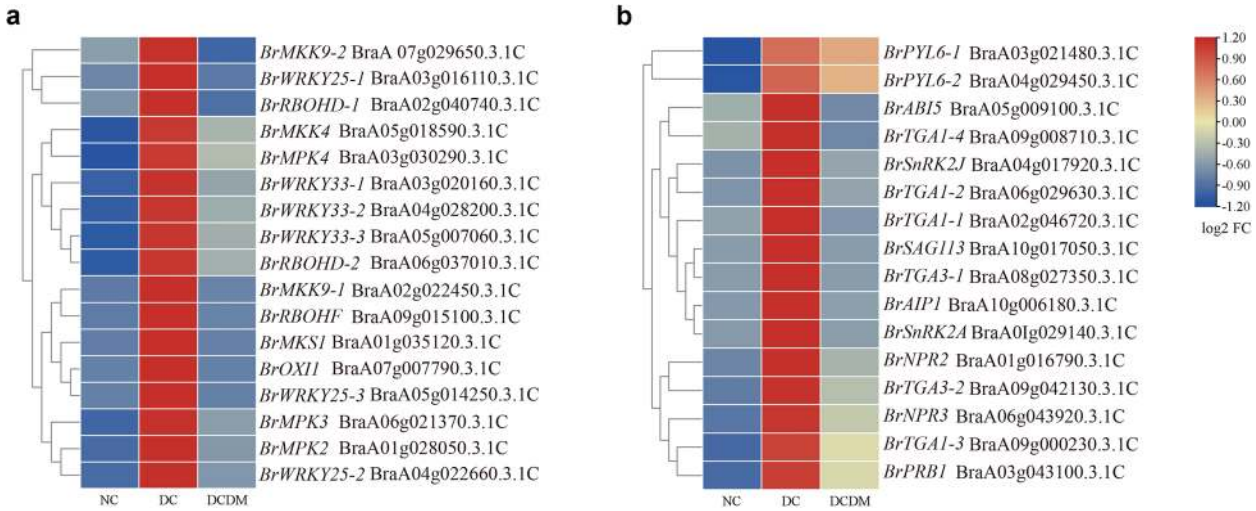


Fig. 8 Heatmap showing expression patterns of differentially expressed genes (DEGs) related to the mitogen-activated protein kinase (MAPK) signaling pathway (**a**) and plant hormone signal transduction pathway (**b**). Expression values from RNA-seq data were log_2-transformed (log_2fold change, log_2 FC) and are displayed as color gradients from blue to red. *BrMKK*s, *Brassica rapa mitogen-activated map kinase kinases*; *BrRBOHD*s, *respiratory burst oxidase homologs*; *BrMPK*s, *mitogen-activated protein kinases*; *BrMKS*s, *map kinase substrates*; *BrOXI*s, *oxidative signal-inducible genes*; *BrPYL*, *pyrabactin resistance 1-like genes*; *BrABI*s, *ABA-insensitive genes*; *BrTGA*s, *TGACG-binding factors*; *BrSnRK*s, *SNF1-related protein kinases*; *BrSAG*s, *senescence-associated genes*; *BrAIP*s, *ABI3-interacting proteins*; *BrNPR*s, *nonexpressor of pathogenesis-related genes*; *BrPRB*s, *basic pathogenesis-related proteins*

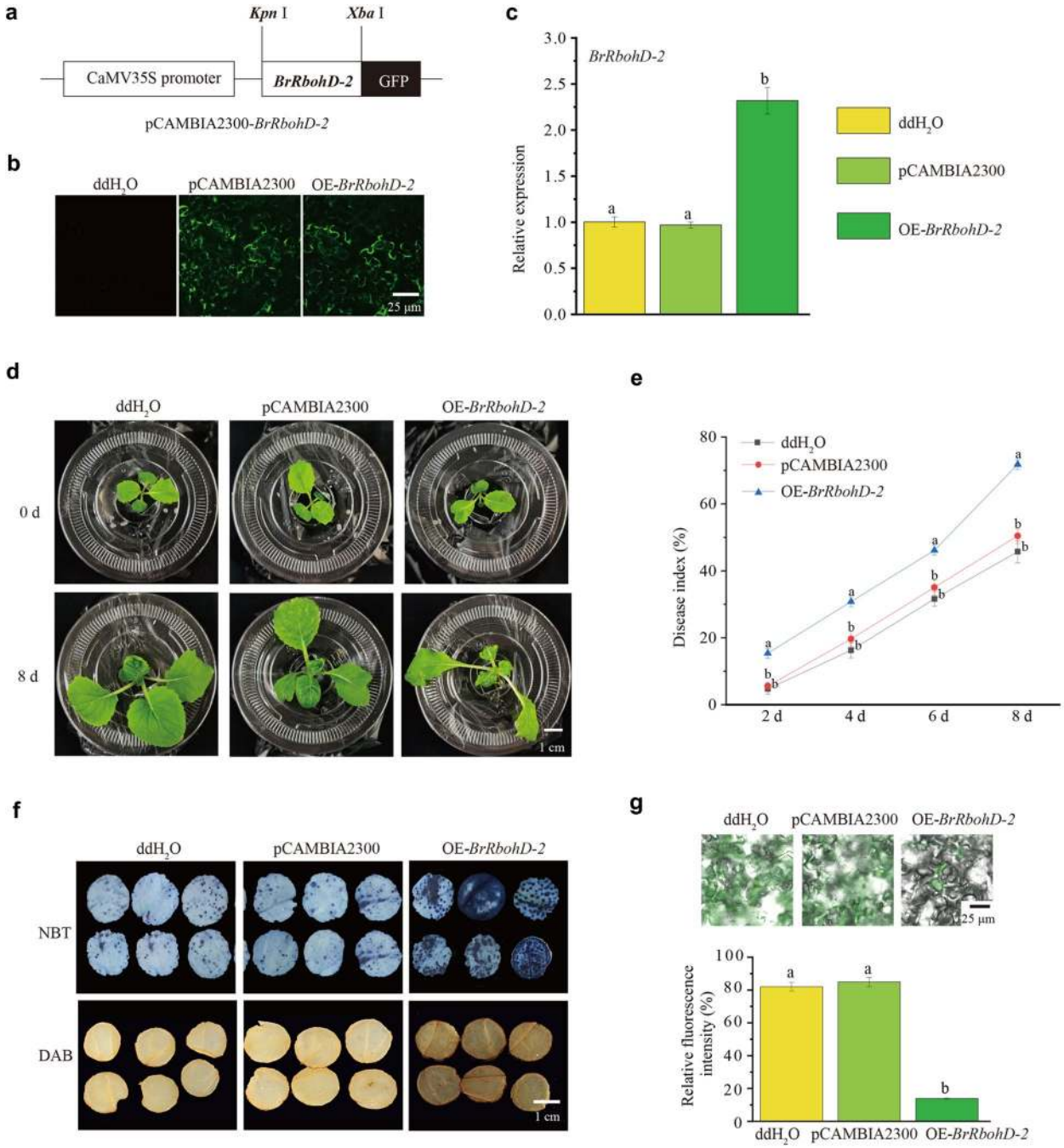


Fig. 9 Phenotypic analysis of *Brassica rapa respiratory burst oxidase homolog D-2* (*BrRbohD-2*)-overexpressing (OE-*BrRbohD-2*) seedlings under Ca^{2+} deficiency stress. **a** Schematic diagram of the pCAMBIA2300-*BrRbohD-2* vector. **b** Observation of green fluorescent protein (GFP) fluorescence in *BrRbohD-2*-overexpressing seedlings. **c** Validation of *BrRbohD-2* expression. **d** Tip-burn phenotype in *BrRbohD-2*-overexpressing seedlings. **e** Disease index of tip-burn. **f** Nitroblue tetrazolium (NBT) and 3,3′-diaminobenzidine (DAB) staining. **g** Cytosolic Ca^{2+} levels in heart leaves. Scale bars = 25 μm (**b**, **g**) and 1 cm (**d**, **f**). Different letters indicate significant differences at $P < 0.05$. Data are presented as the mean ± SEM of three independent replicates

OE-*BrRbohD-2* leaves compared with controls (Fig. 9g). These results suggest that overexpression of *BrRbohD-2* aggravates Ca^{2+} deficiency-induced tip burn in Chinese cabbage seedlings.

Furthermore, the expression of *BrRbohD-2* was silenced using VIGS, and *BrPDS*-silenced seedlings exhibiting photobleaching and leaf shrinkage phenotypes were used to validate successful infection (Fig. 10a;

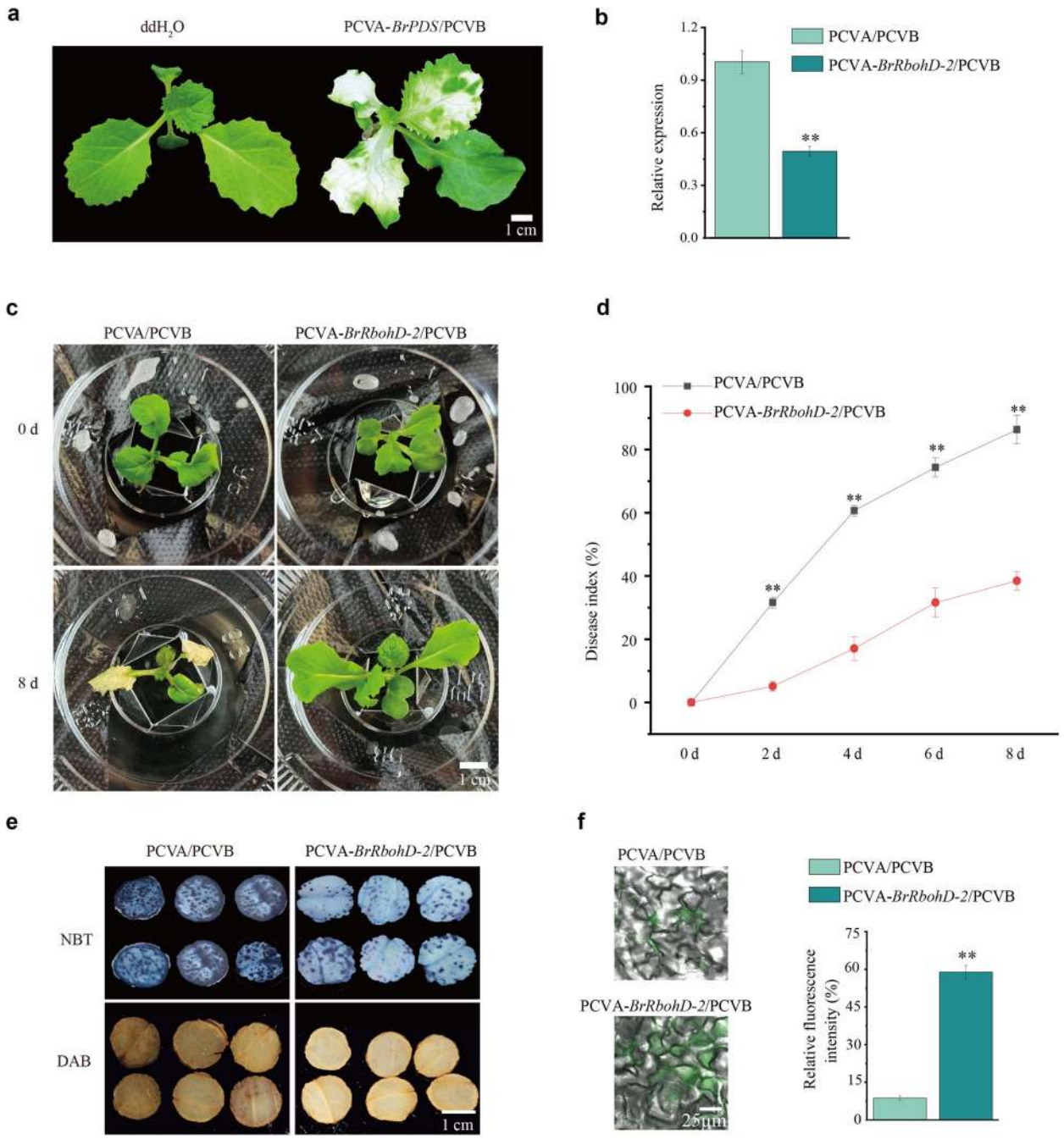


Fig. 10 Silencing of *BrRbohD-2* in Chinese cabbage (*Brassica rapa*) seedlings. **a** Phenotypes of the *phytoene desaturase* (*BrPDS*)-silenced seedlings. **b** Validation of *BrRbohD-2* expression in PCVA-*BrRbohD-2*/PCVB plants. **c** Phenotypes of PCVA/PCVB (control) and PCVA-*BrRbohD-2*/PCVB plants after 0.1 mM Ca^{2+} deficiency treatment. **d** Disease index of tip burn. **e** Nitroblue tetrazolium (NBT) and 3,3-diaminobenzidine (DAB) staining. **f** Cytosolic Ca^{2+} levels in heart leaves. * $P < 0.05$, ** $P < 0.01$. Scale bars = 1 cm (**a**, **c**, **e**) and 25 μm (**f**). Data are presented as the mean ± SEM of three independent replicates

Xiao et al. 2020; Li et al. 2024). Compared with the control group injected with the PCVA/PCVB vector, PCVA-*BrRbohD-2*/PCVB-infected Chinese cabbage seedlings showed reduced expression of *BrRbohD-2* (Fig. 10b), confirming successful gene silencing. Under Ca^{2+} deficiency conditions, *BrRbohD-2*-silenced seedlings exhibited alleviated tip-burn symptoms and reduced DI (Fig. 10c, d). Additionally, NBT and DAB staining intensity was reduced, whereas cytosolic Ca^{2+} levels increased in *BrRbohD-2*-silenced leaves (Fig. 10e, f). These results indicate that silencing *BrRbohD-2* alleviates Ca^{2+} deficiency-induced tip burn in Chinese cabbage seedlings.

Discussion

Tip burn, also known as leaf tip necrosis, is a Ca^{2+}-related physiological disorder that severely affects the quality and yield of *Brassica* leafy vegetables (Lee et al. 2013; Kuronuma and Watanabe 2021). Its occurrence is primarily associated with Ca^{2+} deficiency and inadequate Ca^{2+} delivery to rapidly growing leaf apices (Su et al. 2019). Ca^{2+} is an essential macronutrient in plants, but its mobility from older tissues to developing organs is highly limited. It plays a crucial structural and signaling role in cell walls and membranes, thereby maintaining normal physiological functions under abiotic stress conditions (Zhu 2016; Yuan et al. 2025). Under Ca^{2+} deficiency, plants exhibit impaired growth and development, often accompanied by severe parenchymal cell necrosis (Li et al. 2022; Yuan et al. 2025). Furthermore, proper Ca^{2+} transport across cellular membranes is essential for maintaining intracellular Ca^{2+} homeostasis (Demidchik et al. 2018). Consequently, many studies have focused on elucidating Ca^{2+} uptake and transport mechanisms to develop strategies for mitigating Ca^{2+}-deficiency-related disorders in vegetables.

Chinese cabbage (*Brassica rapa* ssp. *pekinensis*) is an economically important leafy vegetable worldwide, and tip burn is one of its most prevalent physiological disorders, significantly limiting production and quality (Su et al. 2019; Yuan et al. 2025). Despite its agronomic importance, the physiological and molecular mechanisms underlying tip burn susceptibility remain incompletely understood. In this study, we used a tip-burn-susceptible line ('10S42') and a resistant line ('10S27') of Chinese cabbage to investigate the physiological basis of tip burn and identify key regulatory factors involved in this disorder.

Ca^{2+} deficiency severely inhibits growth and induces physiological disorders in *Brassica* species, leading to typical tip-burn symptoms (Li et al. 2022; Zhang et al. 2022; Cui et al. 2023). In this study, Chinese cabbage seedlings of both '10S27' and '10S42' exhibited typical tip-burn symptoms under Ca^{2+} deficiency, including withered leaf margin, heart leaf curling, and heart leaf shrinkage and wilting, consistent with previous reports (Li et al. 2022; Cui et al. 2023). Overall, tip burn significantly reduces vegetable growth and yield (Su et al. 2016; Kuronuma and Watanabe 2021). In the present study, shoot and root fresh weights of Chinese cabbage plants significantly decreased under Ca^{2+} deficiency stress, accompanied by marked reductions in maximum leaf area, root length, and root activity. These results indicate that Ca^{2+} deficiency-induced tip burn severely affects plant biomass accumulation. Moreover, the DI of tip burn significantly increased at 0.25 mM Ca^{2+} and was higher in '10S42' than in '10S27,' indicating differential sensitivity of the two lines to Ca^{2+} deficiency stress.

Photosynthesis is one of the most sensitive physiological processes in plants under stress (Chaves et al. 2009). Leaf chlorophyll content is closely associated with photosynthetic performance, and changes in photosynthetic parameters are key indicators of stress responses (Li et al. 2022; Zhang et al. 2022). In this study, total chlorophyll and carotenoid contents significantly decreased, reflecting the impact of Ca^{2+} deficiency on pigment accumulation in Chinese cabbage seedlings. Similarly, photosynthetic rate and chlorophyll fluorescence parameters also decreased under Ca^{2+}-deficient conditions. These results indicate that decreased chlorophyll content and impaired photosynthetic performance are positively associated with reduced photosynthetic capacity, which may contribute to tip-burn severity and ultimately affect plant growth.

Tip-burn injury occurs in young leaves, which contain lower Ca^{2+} levels than older leaves; thus, Ca^{2+} deficiency in developing leaves is considered a key factor leading to tip burn (White and Broadley 2003). Plants exhibiting tip burn not only show typical symptoms at the margins of young developing leaves, where Ca^{2+} levels are particularly low, but also display an unbalanced distribution of major macronutrient cations (Lee et al. 2013; Kuronuma and Watanabe 2021). In this study, Ca^{2+} distribution and Mn^{2+} content were analyzed across different tissues. The results showed that Ca^{2+} concentration was higher in the tip-burn-resistant line '10S27' than in the susceptible line '10S42.' Moreover, the lowest levels of Ca^{2+} and Mn^{2+} were detected in the heart leaf apex, the primary tissue affected by Ca^{2+} deficiency (Su et al. 2019; Li et al. 2022; Cui et al. 2023). Tip burn is closely associated with Ca^{2+} uptake and accumulation (Yuan et al. 2018, 2021). Furthermore, Ca^{2+} deficiency reduced cytosolic Ca^{2+} concentration in the heart leaf apex, but increased it in roots, where a significant decrease in root activity was observed. These findings suggest that Ca^{2+} deficiency stress may impair Ca^{2+} transport from roots to shoots, leading to localized Ca^{2+} deficiency in young leaves—especially in

the heart leaf apex—thereby increasing the incidence of tip burn in Chinese cabbage seedlings.

The formation and elimination of ROS in plants are maintained in a dynamic balance, whereas Ca^{2+} deficiency disrupts this equilibrium (Carassay et al. 2012; Ali et al. 2023). Plants have evolved physiological and metabolic mechanisms to maintain cellular homeostasis, which is characterized by a basal level of ROS (Nadarajah 2020; Mittler et al. 2022). However, excessive ROS accumulation disrupts homeostasis, leading to oxidative stress and cellular toxicity (Chapman et al. 2019; Nadarajah 2020). Ca^{2+} deficiency, which causes bitter pit in apple, significantly enhances ROS production and reduces antioxidant capacity (Sun et al. 2022). Similarly, in tomato, ROS play a key role in Ca^{2+}-deficiency-related blossom-end rot, where Ca^{2+} imbalance strongly influences disease severity (Topcu et al. 2022). In this study, H_2O_2 and MDA contents increased under Ca^{2+} deficiency in both '10S27' and '10S42,' and NBT and DAB staining showed consistent responses, confirming enhanced ROS accumulation under stress. These results indicate that Ca^{2+}-deficiency-induced ROS accumulation contributes to the development of tip burn in Chinese cabbage seedlings. Moreover, correlation analysis of 24 physiological parameters revealed that H_2O_2 was negatively correlated with DI, highlighting a strong association between ROS levels and Ca^{2+}-deficiency-induced tip burn. Overall, these findings are consistent with previous reports (Topcu et al. 2022; Leong et al. 2023; Li et al. 2023). As key signaling molecules involved in numerous physiological pathways, ROS represent an important area of research. However, Ca^{2+} deficiency stress is known to induce excessive ROS accumulation, leading to oxidative damage (Li et al. 2022; Topcu et al. 2022). Therefore, in this study, DMTU was applied to mitigate abnormal ROS accumulation in Chinese cabbage seedlings under Ca^{2+} deficiency conditions. As expected, DMTU application alleviated tip-burn severity, and the DI was significantly lower in both the $CaCl_2$ and DMTU treatments compared with the Ca^{2+} deficiency treatment alone. Notably, the critical photosynthetic parameters improved, and cytosolic Ca^{2+} levels in leaves were partially restored following treatment. These results strongly suggest that Ca^{2+} deficiency-induced tip burn is closely associated with excessive ROS accumulation (Li et al. 2023; Mukherjee et al. 2023; Kolupaev et al. 2024).

To counteract the adverse effects of abiotic stress, plants have evolved multiple protective mechanisms, including efficient scavenging of excess ROS to alleviate stress-induced cellular damage (Nadarajah 2020; Fedoreyev 2024; Wang et al. 2024). The alleviation of Ca^{2+} deficiency-induced tip burn by DMTU is also associated with the maintenance of Ca^{2+} homeostasis. Importantly, various transport proteins and oxidases have been reported to participate in Ca^{2+} uptake, intracellular distribution, and ROS regulation (Demidchik et al. 2018; Zhang et al. 2022). The influx and efflux of Ca^{2+} across the cellular membrane depend on multiple transporters that collectively regulate cytosolic Ca^{2+} homeostasis (Demidchik et al. 2018). Among these, ACA and CAX proteins are well-characterized tonoplast-localized transporters that primarily mediate Ca^{2+} sequestration into vacuoles (Fuglsang and Palmgren 2021). In *Arabidopsis*, *aca4*/*11* double mutants exhibit elevated basal Ca^{2+} levels and enhanced Ca^{2+} signaling amplitudes compared with wild-type plants, highlighting their key role in intracellular Ca^{2+} regulation (Hilleary et al. 2020). Similarly, the *cax1*/*cax3* double knockout leads to leaf and shoot tip necrosis (Cheng et al. 2005). In addition, *ECA3* plays a crucial role in maintaining Ca^{2+}/Mn^{2+} homeostasis between the cytoplasm and the endoplasmic reticulum (Li et al. 2008). In the present study, RNA-seq analysis identified eight DEGs associated with Ca^{2+} transport proteins, among which *BrACA4*, *BrACA11*, *BrCAX1-1*, *BrCAX1-2*, and *BrCAX3* were significantly downregulated in the DCDM treatment group. In contrast, *BrCNGC2* and *BrCNGC4* were upregulated, suggesting enhanced Ca^{2+} influx into the cytosol in the NC and DCDM groups. Overall, the expression patterns of key Ca^{2+} transporters were consistent with altered cytosolic Ca^{2+} homeostasis, reflecting reduced Ca^{2+} availability in the cytosolic matrix, and ultimately contributing to aggravated tip-burn symptoms.

ROS serve as crucial signaling molecules that regulate plant responses to diverse abiotic stresses, including Ca^{2+} deficiency (Chapman et al. 2019; Nadarajah 2020). Several metabolic processes, along with NADPH oxidases (*RBOHS*), initiate complex signaling cascades that enable plants to adapt to adverse environmental conditions (Chapman et al. 2019; Li et al. 2019). *RBOH* genes play pivotal roles in regulating ROS production and represent key enzymatic sources of ROS in plants (Chapman et al. 2019; Li et al. 2019). In this study, transcriptome analysis revealed that the MAPK signaling pathway was significantly enriched with DEGs. In addition, three NADPH oxidase-related DEGs, namely *BrRbohD-1*, *BrRbohD-2*, and *BrRbohF*, were identified. In particular, *BrRbohD-2* expression was significantly upregulated in the DC group compared with the NC and DCDM groups, suggesting that enhanced *BrRbohD-2* expression is closely associated with Ca^{2+} deficiency-induced tip burn. Studies in various plant species have revealed *RBOHD* functions as a key regulator of ROS production, particularly in H_2O_2 accumulation (Kadota et al. 2015). In oilseed rape,

upregulation of *RbohD* and *RbohF* has been reported to promote ROS accumulation and accelerate leaf senescence (Yang et al. 2018). Similarly, heterologous overexpression of *Cucumis melo RBOHD* (*CmRBOHD*) in *Arabidopsis thaliana* leads to excessive H_2O_2 production (Guo et al. 2023), while elevated expression of *RsRbohD1* in radish (*Raphanus sativus* L.) is associated with ROS accumulation and physiological disorders (Gong et al. 2024). In this study, overexpression of *BrRbohD-2* was associated with a higher DI of tip burn in '10S42' seedlings under Ca^{2+} deficiency stress. In addition, H_2O_2 and $O_2^{\bullet-}$ levels increased, whereas cytosolic Ca^{2+} concentration decreased in the treatment group compared with the control. These results are consistent with RNA-seq data showing that *BrRbohD-2* upregulation under Ca^{2+} deficiency stress. Similarly, previous studies in tomato have reported that Ca^{2+} deficiency is associated with increased ROS accumulation, enhanced NADPH oxidase activity, and a higher incidence of blossom-end rot (Mestre et al. 2012). More importantly, VIGS of *BrRbohD-2* significantly reduced tip-burn DI, decreased H_2O_2 and $O_2^{\bullet-}$ levels, and increased cytosolic Ca^{2+} concentration under Ca^{2+} deficiency stress. Overall, these results indicate that *BrRbohD-2* aggravates Ca^{2+} deficiency-induced tip burn in Chinese cabbage by promoting ROS accumulation.

Conclusions

In this study, seedlings of the susceptible Chinese cabbage line '10S42' and the resistant line '10S27' exhibited tip burn under Ca^{2+}-deficient conditions. The results clarified the physiological and molecular mechanisms underlying Ca^{2+} deficiency-induced tip burn in Chinese cabbage. Ca^{2+} deficiency stress reduced cytosolic Ca^{2+} levels, impaired photosynthetic performance, and triggered ROS accumulation, whereas these symptoms could be alleviated by spraying the ROS scavenger DMTU. Under Ca^{2+} deficiency stress, disruption of ROS homeostasis was accompanied by significant changes in the expression of Ca^{2+} transport-related genes, including *BrACA4*, *BrACA11*, *BrECA3*, *BrCAX1-1*, *BrCAX1-2*, *BrCAX3*, *BrCNGC2*, and *BrCNGC4*. More importantly, Ca^{2+} deficiency stress induced the upregulation of *BrRbohD-2*. Functional analyses through overexpression and silencing of *BrRbohD-2* strongly supported its critical role in linking Ca^{2+} deficiency to ROS accumulation and tip-burn development. Overall, these findings provide valuable insights into the molecular basis of Ca^{2+} deficiency-related disorders in Chinese cabbage and suggest that *BrRbohD-2* is a promising target for improving resistance to Ca^{2+} deficiency stress.

Supplementary Information

The online version contains supplementary material available at https://doi.org/10.1007/s44281-026-00105-x.

Additional file 1: Figure S1. Statistics of growth-related indices of Chinese cabbage at 20 d after Ca^{2+} deficiency stress. a–e Root length phenotype (a), Root length statistics (b), Root activity (c, d), Maximum leaf area (e). Different letters indicate significant differences at $P < 0.05$. Data are presented as the mean ± SEM of three independent replicates.

Additional file 2: Figure S2. Effect of dimethylthiourea (DMTU) spraying on Ca^{2+} deficiency-induced tip burn in '10S27' Chinese cabbage. a Tip-burn phenotype of seedlings after $CaCl_2$ and DMTU treatments under Ca^{2+} deficiency stress. b Disease index of tip burn. c Shoot fresh weight. d Net photosynthetic rate (Pn), maximum quantum efficiency of PSII (Fv/Fm), photochemical quenching (qP), and non-photochemical quenching (NPQ) values. Scale bar = 3 cm (a). Different letters indicate significant differences at $P < 0.05$. Data are presented as the mean ± SEM of three independent replicates.

Additional file 3: Figure S3. Gene Ontology (GO) enrichment (a–c) and Kyoto Encyclopedia of Genes and Genomes (KEGG) enrichment (d–f) analyses in '10S42' Chinese cabbage under Ca^{2+} deficiency.

Additional file 4: Table S1 Primer sequences used for reverse transcription quantitative PCR (RT–qPCR) analysis. Table S2 Summary of RNA-seq data for Chinese cabbage '10S42.' Table S3 Information on differentially expressed genes (DEGs) related to Ca^{2+}-binding proteins and Ca^{2+} transport-associated proteins. Table S4 Information on DEGs related to the mitogen-activated protein kinase (MAPK) signaling and plant hormone signal transduction pathways.

Acknowledgements

We thank Prof. Changwei Zhang (College of Horticulture, Nanjing Agricultural University, Nanjing, China) and Prof. Baohua Li (College of Horticulture, Northwest A&F University, Yangling, China) for providing the PCVA/PCVB vectors, and also thank Dr. Yangyang Yuan and Dr. Jing Zhang from Horticulture Science Research Center, Northwest A&F University at Yangling, for their technical supports in this work.

Author's contributions

HL and SSN conceived and designed the experiments; HL, GQD, and HWC performed the experiments; HL and SGM analyzed the data; MTM and XJK prepared the study materials; HL wrote the manuscript; SSN revised the manuscript. All authors have read and approved the final manuscript.

Funding

This work was supported by the National Natural Science Foundation of China (31801869), the Shaanxi Province Agricultural Science and Technology Key Technology (AK2025-06), and the Natural Science Basic Research Program in Shaanxi Province of China (2023-JC-YB-184).

Data availability

The datasets will be available on reasonable request.

Declarations

Ethics approval and consent to participate

Not applicable.

Consent for publication

Not applicable.

Competing interests

The authors declare that they have no competing interests.

Received: 27 November 2025 Revised: 22 January 2026 Accepted: 25 January 2026
Published online: 20 May 2026

References

Ali S, Tyagi A, Bae H. ROS interplay between plant growth and stress biology: challenges and future perspectives. Plant Physiol Biochem. 2023;203:108032. https://doi.org/10.1016/j.plaphy.2023.108032.

Aloni B, Pressman E. The effects of salinity and gibberellic acid on blackheart disorder in celery(Apium graveolens L.). J Hortic Sci. 1987;62:205–9. https://doi.org/10.1080/14620316.1987.11515770.

Bai H, Chen J, Gao T, Tang Z, Li H, Gong S, et al. A Na^+/H^+ antiporter localized on the Golgi-to-vacuole transport system from *Camellia sinensis*, CsNHX6, plays a positive role in salt tolerance. Sci Hortic. 2023;309:111704. https://doi.org/10.1016/j.scienta.2022.111704.

Berridge MJ, Bootman MD, Roderick HL. Calcium signalling: dynamics, homeostasis and remodelling. Nat Rev Mol Cell Biol. 2003;4:517–29. https://doi.org/10.1038/nrm1155.

Bose J, Rodrigo-Moreno A, Shabala S. ROS homeostasis in halophytes in the context of salinity stress tolerance. J Exp Bot. 2014;65:1241–57. https://doi.org/10.1093/jxb/ert430.

Carassay LR, Bustos DA, Golberg AD, Taleisnik E. Tipburn in salt-affected lettuce (*Lactuca sativa* L.) plants results from local oxidative stress. J Plant Physiol. 2012;169:285–93. https://doi.org/10.1016/j.jplph.2011.10.004.

Chapman JM, Muhlemann JK, Gayomba SR, Muday GK. RBOH-dependent ROS synthesis and ROS scavenging by plant specialized metabolites to modulate plant development and stress responses. Chem Res Toxicol. 2019;32:370–96. https://doi.org/10.1021/acs.chemrestox.9b00028.

Chaves MM, Flexas J, Pinheiro C. Photosynthesis under drought and salt stress: regulation mechanisms from whole plant to cell. Ann Bot. 2009;103:551–60. https://doi.org/10.1093/aob/mcn125.

Cheng NH, Pittman JK, Shigaki T, Lachmansingh J, LeClere S, Lahner B, et al. Functional association of *Arabidopsis CAX1* and *CAX3* is required for normal growth and ion homeostasis. Plant Physiol. 2005;138:2048–60. https://doi.org/10.1104/pp.105.061218.

Costa A, Navazio L, Szabo I. The contribution of organelles to plant intracellular calcium signalling. J Exp Bot. 2018;69:4175–93. https://doi.org/10.1093/jxb/ery185.

Cui S, Liu H, Wu Y, Zhang L, Nie S. Genome-wide identification of *BrCAX* genes and functional analysis of *BrCAX1* involved in Ca^{2+} transport and Ca^{2+} deficiency-induced tip-burn in Chinese cabbage (*Brassica rapa* L. ssp. *pekinensis*). Genes. 2023;14:1810. https://doi.org/10.3390/genes14091810.

Demidchik V, Shabala S, Isayenkov S, Cuin TA, Pottosin I. Calcium transport across plant membranes: mechanisms and functions. New Phytol. 2018;220:49–69. https://doi.org/10.1111/nph.15266.

Fedoreyeva LI. ROS as signaling molecules to initiate the process of plant acclimatization to abiotic stress. Int J Mol Sci. 2024;25:11820. https://doi.org/10.3390/ijms252111820.

Fuglsang AT, Palmgren M. Proton and calcium pumping P-type ATPases and their regulation of plant responses to the environment. Plant Physiol. 2021;187:1856–75. https://doi.org/10.1093/plphys/kiab330.

Gong Q, Wang C, Fan W, Li S, Zhang H, Huang Z, et al. *RsRbohD1* plays a significant role in ROS production during radish pithiness development. Plants Basel. 2024;13:1386. https://doi.org/10.3390/plants13101386.

Guo Y, Zhu J, Liu J, Xue Y, Chang J, Zhang Y, et al. Melatonin delays ABA-induced leaf senescence *via* H_2O_2-dependent calcium signaling. Plant Cell Environ. 2023;46:171–84. https://doi.org/10.1111/pce.14482.

He J, Rössner N, Hoang MTT, Alejandro S, Peiter E. Transport, functions, and interaction of calcium and manganese in plant organellar compartments. Plant Physiol. 2021;187:1940–72. https://doi.org/10.1093/plphys/kiab122.

Hilleary R, Paez-Valencia J, Vens CS, Toyota M, Palmgren M, Gilroy S. Tonoplast-localized Ca^{2+} pumps regulate Ca^{2+} signals during pattern-triggered immunity in *Arabidopsis thaliana*. Proc Natl Acad Sci U S A. 2020;117:18849–57. https://doi.org/10.1073/pnas.2004183117.

Ho LC, White PJ. A cellular hypothesis for the induction of blossom-end rot in tomato fruit. Ann Bot. 2005;95:571–81. https://doi.org/10.1093/aob/mci065.

Huo J, Zhang N, Gong Y, Bao Y, Li Y, Zhang L, et al. Effects of different light intensity on leaf color changes in a Chinese cabbage yellow cotyledon mutant. Front Plant Sci. 2024;15:1371451. https://doi.org/10.3389/fpls.2024.1371451.

Jalmi SK, Sinha AK. ROS mediated MAPK signaling in abiotic and biotic stress striking similarities and differences. Front Plant Sci. 2015;6:769. https://doi.org/10.3389/fpls.2015.00769.

Kadota Y, Shirasu K, Zipfel C. Regulation of the NADPH oxidase RBOHD during plant immunity. Plant Cell Physiol. 2015;56:1472–80. https://doi.org/10.1093/pcp/pcv063.

Kolupaev YE, Taraban DA, Karpets YV, Kokorev AI, Yastreb TO, Blume YB, et al. Involvement of ROS and calcium ions in developing heat resistance and inducing antioxidant system of wheat seedlings under melatonin's effects. Protoplasma. 2024;261:975–89. https://doi.org/10.1007/s00709-024-01952-z.

Kudla J, Batistic O, Hashimoto K. Calcium signals: the lead currency of plant immune responses. Plant Cell. 2010;22:541–63. https://doi.org/10.1105/tpc.109.072686.

Kuronuma T, Watanabe H. Identification of the causative genes of calcium deficiency disorders in horticulture crops: a systematic review. Agriculture Basel. 2021;11:906. https://doi.org/10.3390/agriculture11100906.

Kuronuma T, Ando M, Watanabe H. Tip-burn incidence and Ca acquisition and distribution in lisianthus (*Eustoma grandiflorum* (Raf.) Shinn.) cultivars under different Ca concentrations in nutrient solution. Agronomy. 2020;10:216. https://doi.org/10.3390/agronomy10020216.

Lee J, Park I, Lee ZW, Kim SW, Baek N, Park HS, et al. Regulation of the major vacuolar Ca^{2+} transporter genes, by intercellular Ca^{2+} concentration and abiotic stresses, in tip-burn resistant *Brassica oleracea*. Mol Biol Rep. 2013;40:177–88. https://doi.org/10.1007/s11033-012-2047-4.

Leong R, Tan JJ, Koh SS, Wu TY, Ishizaki K, Urano D. G protein signaling and metabolic pathways as evolutionarily conserved mechanisms to combat calcium deficiency. New Phytol. 2023;237:615–30. https://doi.org/10.1111/nph.18561.

Li X, Chanroj S, Wu Z, Romanowsky SM, Harper JF, Sze H. A distinct endosomal Ca^{2+}/Mn^{2+} pump affects root growth through the secretory process. Plant Physiol. 2008;147:1675–89. https://doi.org/10.1104/pp.108.119909.

Li Q, Yang S, Ren J, Ye X, Jiang X, Liu Z. Genome-wide identification and functional analysis of the cyclic nucleotide-gated channel gene family in Chinese cabbage. 3 Biotech. 2019;9:114. https://doi.org/10.1007/s13205-019-1647-2.

Li Y, Ma J, Gao X, Tie J, Wu Y, Tang Z, et al. Exogenous brassinosteroids alleviate calcium deficiency-induced tip-burn by maintaining cell wall structural stability and higher photosynthesis in mini Chinese cabbage. Front Plant Sci. 2022;13:999051. https://doi.org/10.3389/fpls.2022.999051.

Li Y, Wu Y, Tang Z, Xiao X, Gao X, Qiao Y, et al. Exogenous brassinosteroid alleviates calcium deficiency induced tip-burn by regulating calcium transport in *Brassica rapa* L. *ssp. pekinensis*. Ecotoxicol Environ Saf. 2023;251:114534. https://doi.org/10.1016/j.ecoenv.2023.114534.

Li C, Cui J, Shen Y, Zeng Q, Zhang R, Bai X, et al. *BrERF109* positively regulates the tolerances of drought and salt stress in Chinese cabbage. Environ Exp Bot. 2024;223:105794. https://doi.org/10.1016/j.envexpbot.2024.105794.

Ma Y, Berkowitz GA. Multimeric CAX complexes and Ca^{2+} signaling **–** beyond humdrum housekeeping. J Exp Bot. 2017;68:3997–9. https://doi.org/10.1093/jxb/erx227.

McAinsh MR, Pittman JK. Shaping the calcium signature. New Phytol. 2009;181:275–94. https://doi.org/10.1111/j.1469-8137.2008.02682.x.

Mestre TC, Garcia-Sanchez F, Rubio F, Martinez V, Rivero RM. Glutathione homeostasis as an important and novel factor controlling blossom-end rot development in calcium-deficient tomato fruits. J Plant Physiol. 2012;169:1719–27. https://doi.org/10.1016/j.jplph.2012.07.013.

Miller G, Schlauch K, Tam R, Cortes D, Torres MA, Shulaev V, et al. The plant NADPH oxidase RBOHD mediates rapid systemic signaling in response to diverse stimuli. Sci Signal. 2009;2:ra45. https://doi.org/10.1126/scisignal.2000448.

Mittler R, Zandalinas SI, Fichman Y, Van Breusegem F. Reactive oxygen species signalling in plant stress responses. Nat Rev Mol Cell Biol. 2022;23:663–79. https://doi.org/10.1038/s41580-022-00499-2.

Mukherjee P, Suriyakumar P, Vanchinathan S, Krishnan V, Lal MK, Jha PK, et al. Hydrogen peroxide and GA_3 levels regulate the high night temperature response in pistils of wheat (*Triticum aestivum* L.). Antioxidants. 2023;12:342. https://doi.org/10.3390/antiox12020342.

Nadarajah KK. ROS homeostasis in abiotic stress tolerance in plants. Int J Mol Sci. 2020;21:5208. https://doi.org/10.3390/ijms21155208.

Nie S, Wang R, Li R, Zhang M, Zhang L. Transcriptomic analysis identifies critical signaling components involved in the self-incompatibility response in Chinese cabbage. Sci Hortic. 2019;248:189–99. https://doi.org/10.1016/j.scienta.2019.01.022.

Niekerk LA, Gokul A, Basson G, Badiwe M, Nkomo M, Klein A, et al. Heavy metal stress and mitogen activated kinase transcription factors in plants: exploring heavy metal-ROS influences on plant signaling pathways. Plant Cell Environ. 2024;47:2793–810. https://doi.org/10.1111/pce.14926.

Ravi B, Foyer CH, Pandey GK. The integration of reactive oxygen species (ROS) and calcium signalling in abiotic stress responses. Plant Cell Environ. 2023;46:1037–55. https://doi.org/10.1111/pce.14596.

Robertson DA, Savva GM, Kenny RA. Frailty and cognitive impairment-a review of the evidence and causal mechanisms. Ageing Res Rev. 2013;12:840–51. https://doi.org/10.1016/j.arr.2013.06.004.

Stael S, Wurzinger B, Mair A, Mehlmer N, Vothknecht UC, Teige M. Plant organellar calcium signalling: an emerging field. J Exp Bot. 2012;63:1525–42. https://doi.org/10.1093/jxb/err394.

Su T, Yu S, Yu R, Zhang F, Yu Y, Zhang D, et al. Effects of endogenous salicylic acid during calcium deficiency-induced tipburn in Chinese cabbage (*Brassica rapa L. ssp. pekinensis*). Plant Mol Biol Rep. 2016;34:607–17. https://doi.org/10.1007/s11105-015-0949-8.

Su T, Li P, Wang H, Wang W, Zhao X, Yu Y, et al. Natural variation in a calreticulin gene causes reduced resistance to Ca^{2+} deficiency-induced tipburn in Chinese cabbage (*Brassica rapa* ssp. *pekinensis*). Plant Cell Environ. 2019;42:3044–60. https://doi.org/10.1111/pce.13612.

Sun C, Zhang W, Qu H, Yan L, Li L, Zhao Y, et al. Comparative physiological and transcriptomic analysis reveal *MdWRKY75* associated with sucrose accumulation in postharvest 'Honeycrisp' apples with bitter pit. BMC Plant Biol. 2022;22:71. https://doi.org/10.1186/s12870-022-03453-8.

Swarbreck SM, Colaco R, Davies JM. Plant calcium-permeable channels. Plant Physiol. 2013;163:514–22. https://doi.org/10.1104/pp.113.220855.

Topcu H, Kurek E, Aydın A, Kusvuran S. Melatonin and calcium applications alleviate growth, physiological and nutritional disorders of tomato plants under boron toxicity. Sci Hortic. 2022;304:111324. https://doi.org/10.1016/j.scienta.2022.111324.

Topcu Y, Nambeesan SU, van der Knaap E. Blossom-end rot: a century-old problem in tomato (*Solanum lycopersicum L.*) and other vegetables. Mol Hortic. 2022;2:1. https://doi.org/10.1186/s43897-021-00022-9.

Torres E, Kalcsits L, Nieto LG. Is calcium deficiency the real cause of bitter pit? A review. Front Plant Sci. 2024;15:1383645. https://doi.org/10.3389/fpls.2024.1383645.

Wang C, Luan S. Calcium homeostasis and signaling in plant immunity. Curr Opin Plant Biol. 2024;77:102485. https://doi.org/10.1016/j.pbi.2023.102485.

Wang J, Dou J, Yue Z, Wang J, Chen T, Li J, et al. Effect of hydrogen sulfide on cabbage photosynthesis under black rot stress. Plant Physiol Biochem. 2024;208:108453. https://doi.org/10.1016/j.plaphy.2024.108453.

White PJ, Broadley MR. Calcium in plants. Ann Bot. 2003;92:487–511. https://doi.org/10.1093/aob/mcg164.

Xiao Z, Xing M, Liu X, Fang Z, Yang L, Zhang Y, et al. An efficient virus-induced gene silencing (VIGS) system for functional genomics in *Brassicas* using a cabbage leaf curl virus (CaLCuV)-based vector. Planta. 2020;252:42. https://doi.org/10.1007/s00425-020-03454-7.

Yang L, Ye C, Zhao Y, Cheng X, Wang Y, Jiang YQ, et al. An oilseed rape WRKY-type transcription factor regulates ROS accumulation and leaf senescence in *Nicotiana benthamiana* and Arabidopsis through modulating transcription of *RbohD* and *RbohF*. Planta. 2018;247:1323–38. https://doi.org/10.1007/s00425-018-2868-z.

Yang Y, Tan YQ, Wang X, Li JJ, Du BY, Zhu M, et al. OPEN STOMATA 1 phosphorylates CYCLIC NUCLEOTIDE-GATED CHANNELs to trigger Ca^{2+} signaling for abscisic acid-induced stomatal closure in Arabidopsis. Plant Cell. 2024;36:2328–58. https://doi.org/10.1093/plcell/koae073.

Yuan WL, Yuan SY, Liu ZX, Chen LF, Qiu ZM. Effect of foliar application of $CaCl_2$ on lettuce growth and calcium concentrations with organic and conventional fertilization. HortScience. 2018;53:891–4. https://doi.org/10.21273/HORTSCI13056-18.

Yuan J, Shen C, Yuan R, Zhang H, Xiao Y, Wang X, et al. Identification of genes related to tipburn resistance in Chinese cabbage and preliminary exploration of its molecular mechanism. BMC Plant Biol. 2021;21:567. https://doi.org/10.1186/s12870-021-03303-z.

Yuan J, Shen C, Chen R, Qin Y, Li S, Sun B, et al. *BrCNGC12* and *BrCNGC16* mediate Ca^{2+} absorption and transport to enhance resistance to tipburn in Chinese cabbage. Plant Biotechnol J. 2025;23:2871–87. https://doi.org/10.1111/pbi.70113.

Zhai L, Sun C, Feng Y, Li D, Chai X, Wang L, et al. *Atrop6* is involved in reactive oxygen species signaling in response to iron-deficiency stress in *Arabidopsis thaliana*. FEBS Lett. 2018;592:3446–59. https://doi.org/10.1002/1873-3468.13257.

Zhang S, Gao H, Wang L, Zhang Y, Zhou D, Anwar A, et al. Comparative transcriptome and co-expression network analyses reveal the molecular mechanism of calcium-deficiency-triggered tipburn in Chinese cabbage (*Brassica rapa L. ssp. Pekinensis*). Plants Basel. 2022;11:3555. https://doi.org/10.3390/plants11243555.

Zhu JK. Abiotic stress signaling and responses in plants. Cell. 2016;167:313–24. https://doi.org/10.1016/j.cell.20.

Publisher's Note

Springer Nature remains neutral with regard to jurisdictional claims in published maps and institutional affiliations.